Effects of mechanical compression on the performance of Polymer Electrolyte Fuel Cells and analysis through in-situ characterisation techniques - A review

El Mahdi Khetabi, Khadidja Bouziane, Nada Zamel, Xavier Francois, Yann Meyer, Denis Candusso

Review paper

Effects of mechanical compression on the performance of Polymer Electrolyte Fuel Cells and analysis through in-situ characterisation techniques - A review

El Mahdi KHETABI[1,2,3,4], Khadidja BOUZIANE[1,2,3,4], Nada ZAMEL[5], Xavier FRANÇOIS[3,4], Yann MEYER[2,3], Denis CANDUSSO[1,4]

[1]Laboratoire SATIE (UMR 8029), ENS Paris Saclay, IFSTTAR / COSYS, Université Paris Saclay, Université Paris-Sud. 25 allée des marronniers 78000 Versailles Satory, France.

[2]Sorbonne Universités, Université de Technologie de Compiègne, CNRS, FRE 2012 Roberval, centre de recherche Royallieu, CS 60 319, 60203 Compiègne cedex, France.

[3]Université Bourgogne Franche-Comté, UTBM bât. F, Rue Thierry Mieg, 90010 Belfort Cedex, France.

[4]FCLAB (FR CNRS 3539), Plateforme pile à combustible, UTBM bât. F, Rue Thierry Mieg, 90010 Belfort Cedex, France.

[5]Fraunhofer Institute for Solar Energy Systems ISE, Freiburg, Germany.

Abstract

One of the factors that affect the polymer electrolyte fuel cell (PEFC) performance is the mechanical compression inside the stack. Although this compression plays an important role to ensure efficient gas sealing along with optimised electrical and thermal conductivities during PEFCs operation, excessive mechanical pressure may worsen the fuel cell performance through reducing the porosity and transport ability of PEFC components. In the last few years, intensive research studies have focused on the gas diffusion layers (GDLs) due to the strong relation of their compressibility with the performance of the PEFCs. A few review papers investigating the compression effect on individual fuel cell components have already been published. However, the evaluation of this effect on an operating PEFC has rarely been reviewed. This paper covers a comprehensive overview of the studies that have focused on the relationship between mechanical compression and the observed performance of a PEFC operating in real life conditions (in-situ). In this study, the effects of GDL properties with respect to the applied mechanical compression and the operating conditions are investigated. Much more work in literature has focused on GDL properties. Thus, an extended discussion is dedicated to this cell element in this paper.

Keywords: Polymer electrolyte fuel cell, Assembly pressure, Gas diffusion layer, Optimal clamping pressure, In-situ characterisation techniques, Pressure distribution.

Content

1. Introduction

Global population growth and evolutions in human society have been marked by important increase in energy use and a surging need in power production. These energy requirements have been ensured by fossil fuels since their discovery in the 18th century. However, the combustion of fossil fuels presents serious health and environmental issues as it increases greenhouse gas emissions. Therefore, the need to develop new energy conversion solutions that are more efficient and with minimal pollutant emissions is of paramount importance. In this regard, fuel cells were shown to be one of the most promising technologies for energy conversion. This technology has revealed its potential to substitute non-renewable sources of energy, whether in stationary or mobile applications, with an environmentally friendly energy source [1,2]. In the last few decades, polymer electrolyte fuel cells (PEFCs) have shown their potential for both mobile (e.g. automobile, aerospace, portable) and stationary applications (e.g. micro combined heat and power generation for residential use [3–5]) due to their high efficiency, their low weight and their lower operating temperature (usually between 60 and 80°C [6]). A PEFC is an electrochemical device, as shown in Figure 1, which converts chemical energy from oxygen and hydrogen directly into electrical energy. PEFCs also generate water and heat. State-of-the-art PEFC is composed of different components, including cathode and anode electrodes, where air (or less commonly pure oxygen) and hydrogen are fed as oxidant and fuel, respectively. Other components include: a polymeric membrane, gas diffusion layers (GDL), bipolar plates (BPP), end plates, current collectors, gaskets and commonly a thin layer referred as a microporous layer (MPL) located between the catalyst layers (CL) and the GDL. In order to produce proper electric power, the fuel cells are assembled together by way of mechanical compression using fasteners (e.g. of nuts and bolts). In addition to the assembly pressure, various compression mechanisms take place in operating PEFCs and may affect

their performance. The compression sources associated with each fuel cell component are summarised in Figure 1.

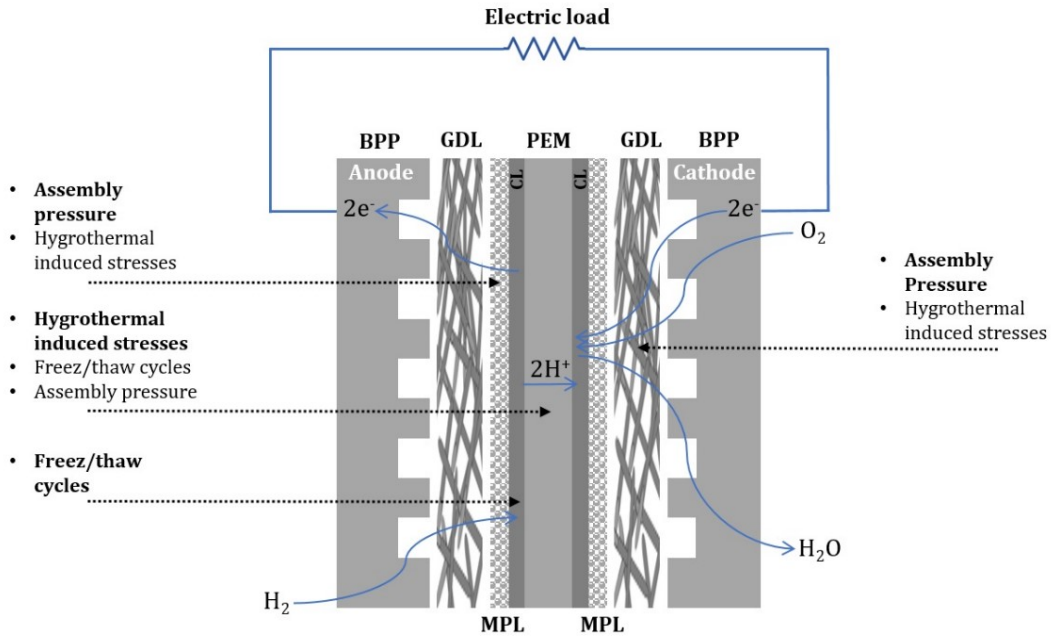

Figure 1. *Different effects of mechanical compression on a PEFC performance; in bold the most important effects on each component.*

Among all the fuel cell components, and from a mechanical point of view, GDLs have attracted much attention in recent years, especially for their strong relationship with the fuel cell performance when it comes to mechanical compression related issues due to their relatively high porous structure (reaching 70% to 85 % [7]). The GDL is a carbon based porous material, generally treated with a hydrophobic agent, e.g. polytetrafluoroethylene (PTFE), to improve its water-repellent characteristics. GDLs play a key role in the diffusion of reactant gases and in the water management. In PEFCs, GDLs need to: (1) - provide pathways for reactant gases from the flow field channels to the catalyst layers; (2) - provide pathways for product water from the catalyst layer to the flow field channels; (3) - electrically connect the catalyst layers to the bipolar plates (BPPs); (4) - conduct heat generated during the electrochemical reactions from the catalyst layers to the BPPs (which have means for heat removal); (5) - mechanically support the MEA; and (6) - homogenise the distribution of the reactants from the BPP channels to the CLs. In order to ensure these functions, the GDL must be: (1) - sufficiently porous to

allow flow of both reactant gases and product water (which have opposite flow directions); (2) - electrically and thermally conductive; and (3) - sufficiently rigid to support the MEA and at the same time flexible to maintain good interfacial contact with the adjacent components. The GDLs are often coated with a MPL to reduce the contact resistance and the mass transport resistance especially at high current densities [8] and mitigate water management issues [9–11]. Various types of GDLs have been reported in the literature, each type having its own characteristics. Figure 2 shows different types of GDLs, namely carbon cloth, carbon paper and felt/spaghetti paper [12].

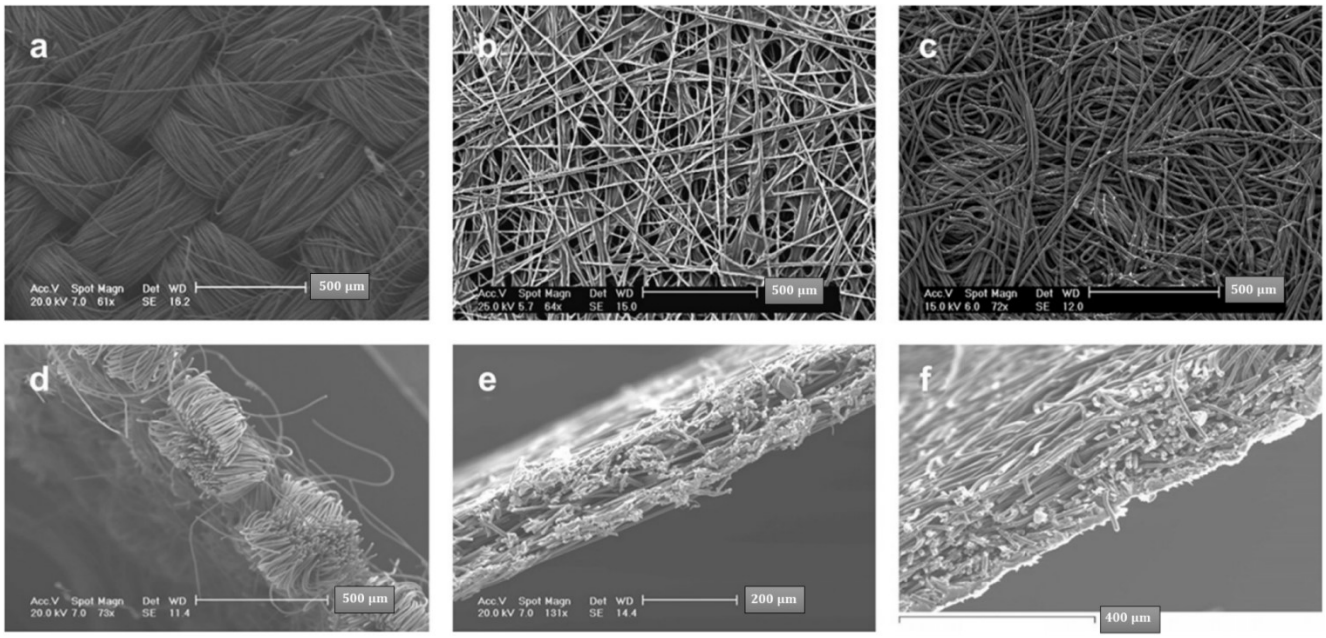

Figure 2. *Different GDL materials a) & d) woven fibres in carbon cloth; b) & e) straight stretched fibres in carbon paper c) & f) felt fibres in carbon paper. Modified from [12].*

Assembling a fuel cell stack requires an accurate control to ensure a good alignment of the stack's individual components, then an appropriate assembly pressure is applied in order to achieve adequate contact between the fuel cell components and to ensure gas-tight operation. In order to prevent hazardous situations, sealing gaskets are generally inserted between the

MEA and the bipolar plates to ensure that no gas leakage (between the fuel cell and its external environment) occurs during the fuel cell operations. Various investigations have been reported in the literature to assess compression characteristics during the assembly process, either by simulations using numerical models [13,14] or experimental investigations using piezoresistive arrays [15,16] or pressure sensitive thin films [17,18]. However, each fuel cell component has its unique characteristics, especially the GDLs. Thus, the assembly pressure depends on these characteristics, which makes difficult to propose a recommended assembly pressure value for PEFCs.

In order to assess the effects of assembly pressure on the fuel cell performance, characterisation techniques for PEFCs have been widely investigated in the literature. Two main types of characterisation are currently employed: (1) - ex-situ, where the individual components are characterised externally to the fuel cell, (2) - and in-situ, where the components are characterised within a fuel cell operating in real life conditions. Through employing these characterisation techniques, a large number of researchers working on the characterisation of PEFCs are placing their focus on some particular issues: (1) - GDL electro-physical properties [19–21]; (2) - mass transport limitations [22–24]; (3) - durability [25–27]; (4) - water transport visualisation techniques [28–30]; and (5) - pressure distribution [15–18]. Due to the complexity of the occurring phenomena, PEFCs must be diagnosed using suitable techniques that allow both evaluating all the presented issues and separating their respective impacts on the overall fuel cell performance.

Until now, numerous characterisation techniques have been reported in the literature to assess the fuel cell performance. A number of reviews focusing on the characterisation techniques for PEFCs have already been reported. Wu et al. [31] presented a review on the diagnostic tools employed in PEFC using electrochemical techniques. Arvay et al. [32] reported a review on the characterisation techniques for GDLs used in PEFCs. Their study focused on the essential properties of GDL, i.e. thermal and electrical conductivity, porosity, pore size, gas permeability, and wettability. The authors regrouped a set of tools used for the evaluation of GDLs by the

use of in-situ and ex-situ characterisation techniques and concluded that the employment of both in-situ and ex-situ techniques is of major importance towards developing high performance GDLs.

Whilst a number of studies in literature have focused on the ex-situ characterisation techniques to investigate the effect of mechanical compression on the fuel cell performance [33–36], others employed both ex-situ and in-situ techniques with less focus on the latter [37,38]. Some review studies have also been reported in the literature so far [39–41]. In all these studies, it was well recognised that mechanical stress is one of the main factors that affects PEFC performance. In a recent review on the effect of mechanical compression and dimensional change analysis on PEFC components [39], special attention has been attributed to the GDLs, and a range of dedicated characterisation methods have been presented. In their manuscript, Millichamp et al. [39] provided a good state-of-the-art review regarding these issues, with an important focus on ex-situ characterisation techniques. A number of clamping methods described in the academic and patent literature has also been presented. However, no direct conclusion was drawn since there were no comparative studies on the different clamping procedures [39]. In a 2018 study, Dafalla and Jiang [40] reported a comprehensive review on the mechanical stresses and their related effects on structural properties of PEFC components and performances. The authors reviewed different sources of stress within the cell and their respective impacts on its performance deterioration as well as the induced structural damages of the fuel cell components. The report concluded that comprehensive understanding of the combined realistic effects of mechanical stresses might be of major influence on the enhancement of fuel cell performance.

Thus far, to the authors' knowledge, no review focusing principally on the effects of mechanical compression on PEFCs operating in real life condition, that is to say on in-situ characterisation techniques, has been reported in the literature. The effects of the generated stresses within an operating fuel cell evaluated by the use of in-situ characterisation technique have not been reviewed so far, even though they might be a key issue towards the improvement of the fuel

cell performance. In this regard, the objectives of this review are to identify and review studies tailored towards the investigation of these effects, to provide a comprehensive overview of the experimental in-situ characterisation techniques and to suggest promising routes for more developed PEFCs characterisation techniques. Based on our review, a summary of the progress made in the investigated field and an outlook for future works are then put forward.

2. Sources of mechanical stress and their respective impacts

Fuel cell stacks require mechanical compression during the assembly process to ensure both good electrical and thermal conductivities, between the stack components, and gas-tight operations. In a PEFC, two major types of compression mechanisms take place, the first is due to external forces, e.g. the applied compression during the assembly process, and the second is caused by internal forces that are generated inside the fuel cell during its operation (e.g. membrane hydration/dehydration, temperature variation, freeze/thaw cycles). In both cases, components within the fuel cell are subjected to compressive forces that may either improve or worsen the fuel cell performance. In this section, compression mechanisms and their respective effects are presented.

It has to be mentioned that in all the coming sections of this review, and for comparison purposes, compression data are preferentially provided in MPa units (which equals to 1 $N.mm^{-2}$). However, in a number of the studies reported in the literature, this information has not been provided or cannot be determined; in these cases, other compression data (e.g. clamping torque, compression ratio) are given.

2.1. Assembly pressure

One of the major sources of mechanical stresses within the fuel cell components is the clamping pressure. The induced stresses are generated during the final operation of the assembly process of the fuel cell stack. Although mechanical compression must be evenly applied onto the fuel cell stack to prevent gas leakage during the fuel cell operation, excessive compression was shown to cause permanent damage to the fuel cell components [42–44]. Compared to other fuel cell components, the GDL is considered to be the component most subjected to structural deformation under compressive loads due to its soft and brittle structure [43,45]. Mason et al. [44] presented a study on the effect of GDL compression on the PEFC performance. It was observed that higher compression not only leads to deformation of carbon fibres, but also to an increasing number of high stress regions between intersecting fibres that causes fibre crushing. Moreover, GDLs can deform differently under the applied compression. Under the channels, the GDL intrudes in the void spaces creating a phenomenon referred to as ‘tenting’. Whereas under the ribs, the GDL is compressed to the gasket thickness [46] and the carbon fibres are crushed. This leads to a decrease in the porosity of the GDL that, in turn, increases mass transport resistance. This resulting loss in the ability to supply the reactant gases to the catalyst layers may induce reactants starvation and could also hinder liquid water from being removed, causing flooding [47]. The Scanning Electron Microscopy (SEM) images shown in Figure 3 depict the compression effect on a carbon paper GDL, with the two regions of compressed and uncompressed material, under the ribs and the channels, respectively. The rib area is visible from region (b), where broken and compacted carbon fibres can be seen. The compression of GDL fibres not only decreases the porosity of the GDL material, but also enlargens internal fibre connections leading to a decrease in the contact resistance. This latter event will be discussed in more detail in the coming sections.

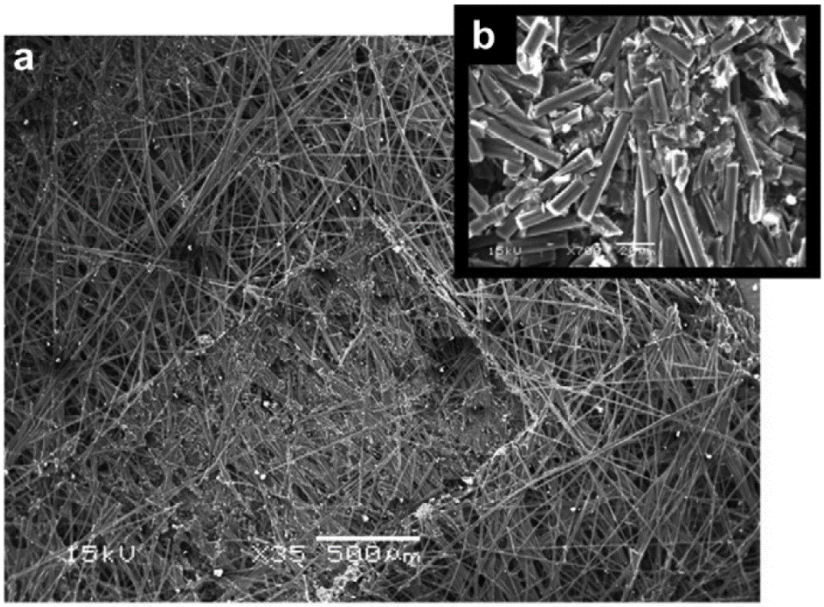

Figure 3. *GDL carbon paper under compression of 12,5 MPa, (a) the impression of the BPP land and (b) broken fibres under the land areas. From [44].*

Khajeh-Hosseini-Dalasm et al. [48] carried out a study on the effects of mechanical compression on a TGP-H-120 Toray paper GDL using the high resolution X-ray Computed Thermography (CT) technique. Under a compression of 3 MPa, a 16% reduction in the average porosity was observed between the region under the rib and the zone under the channels. In addition, a large GDL penetration into the channel was seen as the compression increased, namely 28, 61 and 132 µm were measured under compression of 1, 2 and 3 MPa, respectively. In line with [48], Kandlikar et al. [42] investigated the effects of GDL intrusion into the gas channels of the BPP. The authors reported that as the compression was applied, a part of the GDL protruded into the channels, leading to a partial blockage of the gas channels. Furthermore, it was observed that this intrusion was not uniform for all the gas channels, some major intrusions were witnessed within the channels located at the edges of the BPP. The latter was explained by the location of the assembly bolts that were located at the edges of the PEFC fixture used.

2.1.1. Electrochemical techniques

Electrochemical techniques have been widely employed for in-situ investigations on the effects of mechanical stresses on PEFC performance. Thus far, two familiar methods have been typically reported in the literature covering this area, namely polarisation curves and electrochemical impedance spectroscopy (EIS). In a 2006 study, Ge et al. [49] reported an early use of a fuel cell test fixture allowing in-situ investigations on the effects of mechanical compression on the fuel cell performance. The compression process consisted of a compression plate acting on one fuel cell end-plate. The authors used a single cell with two GDLs (ELAT carbon cloth and Toray carbon fibre paper). It was shown that mechanical compression has a limited impact on the fuel cell performance at low current densities (below 0.8 $A.cm^{-2}$). However, the effect of mechanical compression was more pronounced when the cell was operated at high current densities for both carbon cloth and carbon paper GDLs. This effect was found to be more dominant in the case of the carbon fibre paper GDL (Toray). Figure 4 shows the polarisation curves for the carbon cloth GDL for different compression ratios. As can be seen, at low current densities, the fuel cell performance increased first with increasing the compression ratio (from 40 to 45%), then decreased at high current densities, at which lower compression ratio (14%) gave the best fuel cell performance. Therefore, an optimal compression ratio exists at which the fuel cell reaches its maximum performance. However, this latter was not reported in this study since compression ratios below 14% were not attainable, as the sealing of the fuel cell used could not be ensured at compression ratios lower than this value.

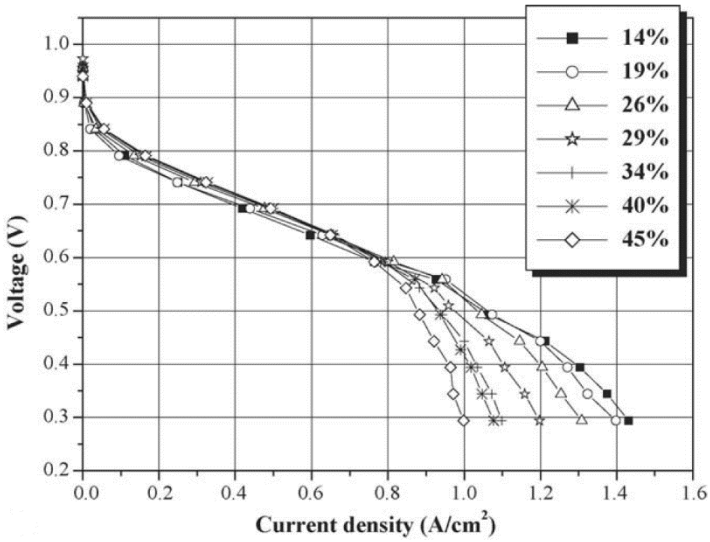

Figure 4. *Polarisation curves for carbon cloth GDL at different compression ratios, at a cell temperature of 65°C, with cathode and anode flow rates of 1200 sccm and 2200 sccm, respectively, with cathode and anode humidifiers temperatures of 80°C. From [49].*

Senthil Velan et al. [50] investigated three carbon cloth GDLs with three compression ratios of 16.6, 22.2, and 30.55%, along with a pristine GDL. It was shown that the GDL with compression ratio of 30.55% showed the worst performance in the high current density region. This finding was attributed to the fact that mechanical compression narrows down the pore size of the GDL and thus hinders reactant from reaching the CL. Moreover, it was reported that higher compressive loads may worsen the water management capability of the fuel cell. According to this study, a 16.6 % compression ratio gave the best performance at fuel cell voltages of 0.15 V and 0.6 V. This finding was attributed to the better pore distribution and the reduced ohmic resistance achieved at this compressive load. Similar results were reported in [51] for a self-humidifying and air breathing PEFC.

Mason et al. [43] carried out a study on the effect of mechanical compression on the PEFC performance using EIS technique. Their experimental setup consisted of a commercially available cell compression unit (Pragma Industries SAS, France), allowing two operating modes, namely controlled compression and controlled displacement with resolutions of 0.01

MPa and 1 μm, respectively. The analysis of the effect of compression on individual loss mechanisms was carried out using EIS measurements (Figure. 5 (a)). The authors reported that as the compression increased, the high frequency intercept of the impedance spectra with the real axis decreased. This was explained exclusively by the reduction in the contact resistance between the GDL and BPP as it was assumed that there was no change in the ohmic response of the electrolyte. Furthermore, it was observed that, simultaneously with the decrease in contact resistance, the charge transfer and mass limitation arcs increased in size. These changes were reported to be solely due to the increase in mass transport resistance. Similar results were reported in [8,52,53]. Figure 5 (b) represents the evolution of the contact resistance and mass transport resistance as a function of the applied compression [43]. The non-linear change in the contact resistance with respect to the applied compression reported in this study agrees well with previously published work [36] using mainly ex-situ techniques to determine the electrical contact resistance between BPP and GDL materials. Throughout the range of compression, the increase in mass transport resistance was seen to be much higher than the decrease in contact resistance, Therefore, the optimum compression point was reported to be the minimum compression that ensures gas sealing and, concurrently, maximum fuel cell performance.

(a)

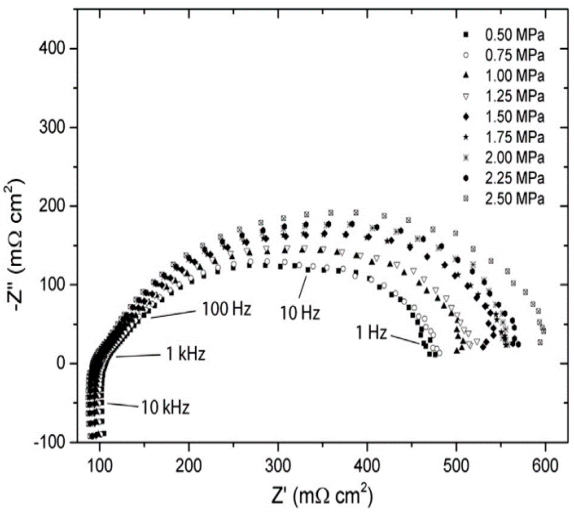

(b)

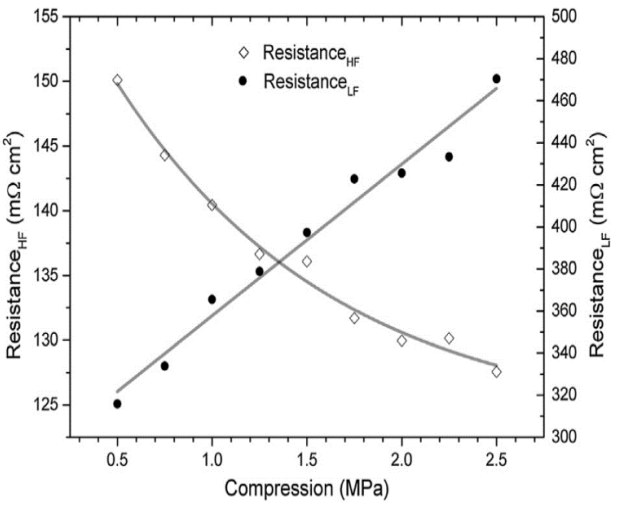

Figure 5. *(a) EIS plots of a PEFC under a mechanical compression ranging from 0.5 to 2.5 MPa, (b) Relationship between the high and the low frequency resistances (*$Resistance_{HF}$ *and* $Resistance_{LF}$*) as a function of the compression (data from (a))* $Resistance_{HF}$ *and* $Resistance_{LF}$ *are proxies for the contact resistance and the mass transport resistance, respectively. From [43].*

Wen et al. [18] presented a study on the effects of the mechanical clamping pressure on both a single cell and a 10 cell PEFC stack. The authors reported that, for either the single cell or the 10 cell stack, a maximum power density was achieved at higher clamping torque. In line with [18], Yim et al. [54] investigated two stacks (5 cell PEFC) with different GDL compression ratios of 15% and 30%. It was observed that the stack with high compression ratio presented a better performance, for all current ranges, compared to the stack with a low compression ratio. This was attributed to the dominance of the decrease in the contact resistance against the increase in mass transport resistance as the applied compression increases.

Ous and Arcoumanis [55] employed a fuel cell compression unit allowing the application of compressive loads from 0.8 to 5 MPa through changing the clamping torque of a central screw. The used PEFC consisted of a single cell with a Toray H-060 GDL. The authors reported that increasing the compression from 0 to 2 MPa improved the fuel cell performance, with greater improvement in the ohmic region compared to the mass transport one. However, as the compression exceeded 5 MPa, the fuel cell performance declined drastically. This result was attributed to two main factors: i) the deflection of the plates in the compression unit used leading to an increase in the internal resistance of the fuel cell, and ii) the decrease in the GDL porosity as the compression loads become more important. Chang et al. [56] investigated a single cell with three GDL types (Sigracet® 10BA, 25BA, and 35BA). The assembly pressure was applied using a test fixture allowing the compression to be applied through a push rod driven by a pneumatic cylinder. For the three GDLs used, it was found that the peak power density reached its maximum at a compression of 3 MPa. The authors reported that higher compression loads (over 3 MPa) resulted in a decrease in the fuel cell performance. This finding was explained by some ex-situ measured changes in the GDL's electro-physical properties (gas permeability, water contact angle and in-plane electrical resistivity) as the

compression exceeded 3 MPa. Similar results were reported in [37,45,57] where a trade-off between the contact resistance and the mass transport resistance was found to give the best fuel cell performance.

A range of studies have been conducted on the effects of assembly pressure through employing both polarisation measurements and EIS technique. Some authors emphasised that higher clamping pressure gives best PEFC performance whereas others reported that minimal clamping pressure, which ensures gas tight operation, needs to be considered for PEFCs. However, most of the studies suggested optimal clamping pressure that gives a trade-off between the reduction in the ohmic resistance and the mass transport resistance after GDL deformation to be most desirable towards achieving high PEFC performance. Nonetheless, the lack of cohesion in the reported studies (clamping methods, operating conditions, PEFC components) makes it hardly possible to draw general conclusions regarding optimal clamping pressure.

2.1.2. Assembly pressure distribution

Various research teams investigated the mechanical pressure distribution in PEFCs. In addition to the assembly pressure, the clamping configuration (e.g. the number of clamping bolts and their positions with respect to the cell geometry) may drastically affect the fuel cell performance. Different PEFC assembly configurations have been reported in literature. For instance, the point-load design has received much attention [14,18,55,58]. In this design, bolt configuration and clamping torque are considered as the most important factors that affect the uniformity of the pressure distribution within the fuel cell components. A well-developed clamping design will minimise the interfacial contact resistance, homogenise the pressure distribution, and ensure gas-tight operation. In contrast, uneven pressure distribution may worsen fuel cell performance or even permanently damage its components, e.g. through the creation of hot spots [52,53] which have detrimental effects on the fuel cell durability. Up to

now, two techniques have been reported in the literature to investigate the pressure distribution in PEFCs, namely the pressure sensitive thin films and the piezoresistive mapping sensors.

Although the investigations on pressure distribution using pressure sensitive films have been used in off-line fuel cells (not operating PEFCs) so far, this technique still provides valuable information regarding the pressure distribution across the fuel cell components. The analysis of the pressure distribution using this technique is based on the principle that as the mechanical compression is applied, microcapsules contained in the pressure sensitive film are broken and a colour-forming material is released and absorbed by the thin film. The released colour intensity indicates the degree of the applied compression. The greater the mechanical compression, the more intense the colour. Since pressure sensitive films have small thicknesses (lower than 200 μm for all compression ranges [59]) compared to the thicknesses of GDLs and the gaskets (e.g. 0.5 mm thickness of the gasket compared to 90 μm for the pressure sensitive film in [18]), it was reported that pressure sensitive films have negligible effect on the internal compression distribution [18]. Thus far, their use to investigate pressure distribution across PEFC components remains suitable.

Wen et al. [18] experimentally investigated the effect of different combinations of clamping torque and bolt configuration on the performance and pressure distribution of a single cell and 10 cell PEFC stack. The authors reported that for both single cell and a 10 cell stack, the pressure distribution uniformity and the maximum power density was improved as the number of bolts and the clamping torque were increased. This finding was explained by the changes of the electrical contact resistance and the GDL porosity under the effect of mechanical compression, meaning that the pressure uniformity was improved and consequently reduced the ohmic resistance of the PEFC, especially the contact resistance, and thus increased the maximum power density. These results are in good agreement with [54,57].

De la Cruz et al. [17] measured the stress distribution in a PEFC stack. The effect of the membrane swelling was investigated by soaking the MEA in liquid water. Afterwards, the MEA was assembled between two pressure sensitive films in a single cell test fixture with a fixed

clamping pressure. It was shown that the pressure distribution in the MEA increased from the centre to the edges. Therefore, the edges of the membrane underwent the highest mechanical stresses. The report concluded that using materials to dissipate high stress concentration at the edges could be an alternative solution to mitigate the inhomogeneous pressure distribution issue.

Bates et al. [60] experimentally investigated the pressure distribution on the GDLs in a 16 cell PEFC stack using various clamping pressures (from 0.5 to 2.5 MPa) and clamping durations. Through a visual analysis of the compressed pressure sensitive films, higher stress regions were observed at the edges compared to the centre of the GDL used. The authors also reported that preloading may be of major impact on the pressure distribution. It was shown that increasing the duration of a load applied at the centre of the endplates resulted in a significant increase in the pressure applied on the GDL. The study concluded that applying a load at the centre of the endplate for a given duration before operating the fuel cell might have some beneficial impacts on the fuel cell performance. Indeed, it allows materials to be settled and the load to be distributed more uniformly over the surface of the stack components. As a matter of fact, fuel cells may be subjected to hundreds of thousands of load cycles during their operational lifetime [61]. With this regard, some authors have already investigated the effects of cyclic loading on the PEFC performance [36,62], it was shown in [36] that the total through-plane resistance of a GDL Sigracet® 24AA decreased upon increasing loading / unloading cycles up to the third cycle, with the first cycle showing the highest decrease up to 50%. Similar results were also reported in [62] where cyclic loading/unloading was shown to decrease the total resistance of a GDL Sigracet® 34BC up to the eighth cycle, with the highest decrease of about 30% occurring during the first cycle.

Gatto et al. [16] investigated the effects of the assembly pressure and gasket materials on PEFC performance and mechanical pressure distribution. The authors employed a pressure mapping sensor (TEKSCAN #5076, USA [63]) that had a pressure resolution of about 10 kPa. A single cell PEFC with a carbon cloth GDL was used. The mechanical compression was

applied through varying the clamping torque on the assembly bolts, ranging from 7 to 13 Nm. With regard to the pressure distribution, it was reported that as the clamping torque increased, the clamping plates of the assembly fixture were deformed leading to an uneven pressure distribution. The centre of the GDL was reported to be less loaded (descending below 0.7 MPa) compared to its edges. The pressure concentration on the edges was shown to rise upon increasing the clamping torque until it reached the saturation level of the sensor used (over 10 MPa in some regions starting from a clamping torque of 7 Nm). Similar results were reported in [15]. Figure 6 depicts the experimental measurements that were carried out using the pressure mapping sensor for different clamping torques. The authors in [16] also emphasised that the gasket material and thickness affect the pressure distribution, for the same assembly pressure, and thus may influence the performance of the PEFC; this latter is in good agreement with results reported in [64,65].

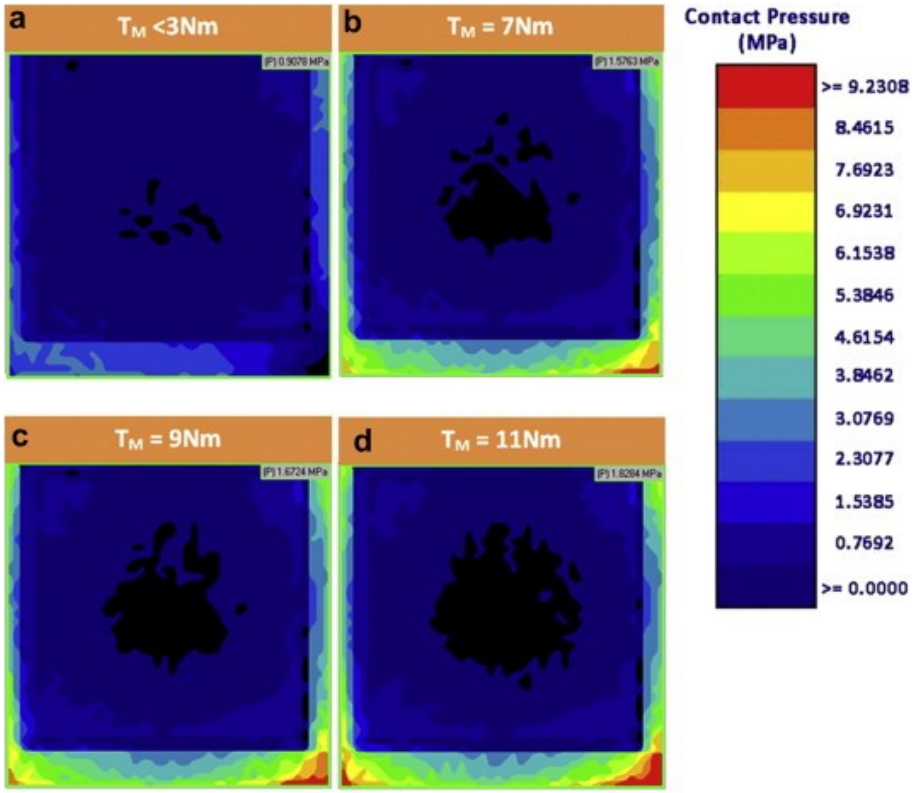

Figure 6. *Pressure maps measured in a PEFC single cell with an active area of 25 cm^2, at clamping torques of (a) <3, (b) 7, (c) 9 and (d) 11Nm, black spots correspond to the regions where the compression descends below the sensitivity of the sensor (< 0.7 MPA). from [16].*

In summary, the reported studies in the literature emphasise that the PEFC clamping process using fasteners induce an inhomogeneous pressure distribution across the fuel cell components. Moreover, it has been well proven that the inhomogeneity increases upon increasing the clamping torque (i.e. higher stress regions on the edges compared to the centre that remains with less compressive load). Therefore, developing new compression methods is of paramount importance in order to reduce the detrimental effects of inhomogeneous pressure distribution on the PEFC performance. Some clamping mechanisms aiming to homogenise the pressure distribution in PEFC stacks have already been reported in the patent literature, e.g. compression retention systems using: external springs [66,67], compliant strapping [68], overlapping sheets [69]. With this regard, Millichamp et al. addressed a range of compression assembly procedures reported in the patent literature in their review [39]. However, studies focusing on the comparison of the reported assembly procedures are still lacking in the literature [39]. This is owing to the fact that almost all the reported studies focused on the pressure distribution in PEFC using the traditional assembly procedure (point-load design using typical fasteners: bolts and nuts). Therefore, future investigations in this area could propose novel optimised clamping methods by including some technical comparisons of the compression retention systems reported in the patent literature.

2.2. Vibration

Although fuel cell assemblies are not a source of induced vibrations due to their compact structure with no moving parts (unlike internal combustion engines), fuel cells are subjected to vibrations caused by the sometimes harsh external environments they are operated in (e.g. applications in light and heavy-duty vehicles, aircraft applications etc.). The frequency of these vibrations may vary depending on the application. For automobile applications, it was assessed that the cell experiences vibrations within the frequency range of 8-16 Hz due to the oscillations of the vehicle wheels and axles along with the non-uniform nature of the road

[70,71]. The effects of vibration on PEFCs have already been investigated in the literature. These effects were assessed under: i) harmonic [72–74], ii) random [75,76], and iii) real-world vibrations [77–81]. The reader can refer to the review study reported by Haji Hosseinloo and Ehteshami [82] for more details on the effects of shock and vibration on PEFC performance and component degradation.

In this study, the reported work related to the effects of real-world induced vibrations on PEFC performance will be discussed. These studies were carried out by investigating the fuel cell performance either during or after the fuel cell operation by means of: i) mounting the fuel cell directly on its final application. ii) placing devices that measure the real multi-directional excitations (e.g. accelerometers) on the final application and then reproducing the same vibration conditions (from an excitation spectrum) in the laboratory using vibrating platforms. Bétournay et al. [83] reported one of the first studies related to this issue. The authors examined the effects of underground mining conditions on fuel cell performance and physical degradation of the fuel cell stack. Vibration tests were carried out over a period of 49h. The results showed that there was neither physical damage nor significant decrease in the fuel cell performance after exposing the fuel cell to vibration/shock during underground driving conditions. Rajalakshmi et al. [76] evaluated the effects of simulated vibrations on the performance and the mechanical integrity of a PEFC stack that was subjected to swept-sine and random excitations for a duration of one and a half hours. Their results showed no significant decrease in the PEFC performance and no changes in individual cell voltages. This latter was attributed to the fact that contact resistance had not increased after the vibration tests.

Hou and co-workers reported a series of experimental studies with regard to the effects of long-term vibrations on fuel cell performance in light-duty vehicles [77–81]. In all the five reported studies, real-world vibrations were first measured on a fuel cell mounted in a vehicle, which was in turn mounted on a road simulation test bench (MAST - Multi-axial Simulation Table). This system allows the simulation of realistic real-world vibrations of a driving vehicle

on real-world roads. Afterwards, the measured excitation spectra was applied to the fuel cell using a six-degrees-of-freedom vibrating platform. During the vibration tests, the fuel cell stack was not in operation; nonetheless, the fuel cell stack was moved to a PEFC test bench within regular periods in order to assess the performance as a function of the progression of the vibration tests. In their earliest study, Hou et al. [77] investigated the effects of vibration on electrical insulation and gas-leakage. After a 150 h vibration test, the hydrogen leakage rate was reported to increase by 50% whereas the insulation resistance of the stack was shown to decrease by 17.5%. They also reported an increase of the ohmic resistance by 55.8% in [78].

In a later study, Hou et al. [79] extended their earlier investigation to examine the cell's steady state efficiency undergoing a 160 h vibration test. The authors reported a decrease of 20% and 5.4% in the fuel cell steady-state efficiency and the maximum efficiency point, respectively. Moreover, a decrease of 30.7% in the hydrogen use was recorded after the vibration test. This was explained by the appearance of pinholes on the membrane caused by the vibration conditions. In another study, Hou el al. [80] examined the effects of vibration on the performance of a PEFC using the EIS technique. The vibration tests were carried out over 200 h. The authors reported an average rise in the ohmic resistance of 0.0357 % per hour. This growth corresponds roughly to a 7.14% increase in the ohmic resistance over the 200 h test duration. Recently, Hou et al. [81] revised the findings reported in their earlier investigations [77–80] with a more developed characterisation process. The test duration was extended to 250 h. Concurrently, the time intervals separating the performance tests were shortened. After the vibration tests, the anode hydrogen leakage rate increased to 1.7 times its initial value. In addition, the rated voltage and the OCV dropped by 3.6% and 0.9%, respectively. Furthermore, the ohmic resistance was shown to increase by 5.4% after vibration tests. The performance degradation was attributed to the increase in the ohmic resistance and the mass transport limitation at high current densities.

Liquid water transport under vibration was investigated in [84] using a transparent cell. Visual inspection of water transport under vibration showed that vibration (a frequency of 20 Hz and

an amplitude of 4mm) could facilitate evacuating liquid water as it reduce water adherence to the surface of the other components. Therefore, operating the fuel cell under specific vibration conditions might be beneficial for water management within the fuel cell; this issue was reported earlier by Palan and co-workers [85,86]. In their first investigation on this topic, Palan and Shepard [85] studied the feasibility of the use of vibrational and acoustical methods to enhance water management of the fuel cell assembly through atomisation of the condensed water droplets in either the BPP gas channels or the MEA. The authors employed numerical simulation and showed that the proposed methods might achieve the required acceleration levels (250 g) to atomise a water droplet having a radius of 2 mm. The report concluded that the proposed method was feasible via appropriate choice of the source strength and the frequency of the excitation. In their second study, Palan et al. [86] theoretically investigated the use of vibrational and acoustical methods to enhance the performance of a PEFC by improving the water removal capacity of the fuel cell components. It was shown that a displacement amplitude of 1 μm on a vibrating BPP can evoke water droplets movement. This might be achieved by the implementation of surface acoustic waves with a minimal parasitic power consumption of 21 mW. This finding seems to be a promising route to mitigate PEFC water management issues. Indeed, recent studies carried out by Ma and co-workers [87–90] investigated the potential use of the so-called piezoelectric polymer electrolyte fuel cells (PZT-PEFCs). In these novel PZT-PEFCs, the piezoelectric actuators are placed on the cathode channels allowing the operation of an air breathing PEFCs by forcing the air into the channels and, at the same time, pumping out water during the compression phase of the PZT device. In their last study [90], the PZT device was stated to require a power of 0.6354 W for a PEFC stack with an optimal power of 4.4981 W and a 60 Hz functioning frequency. This novel technique was shown to mitigate cathode flooding effects and enhance the performance of air breathing fuel cells. However, the proposed techniques in [87–90] are only dedicated to air breathing PEFCs, which are generally suitable for low power portable applications [91–93]. Therefore, new numerical models development and experimental investigations should be

carried out to validate the proposed methods in [85,86] for fuel cells operating with air compressors and humidifiers, which are more likely used in high power PEFC applications.

In summary, a number of research teams studied the effects of vibration-induced stresses on the PEFC performance and component degradation. Some studies concluded that vibration had beneficial impacts on the fuel cell performance whereas others reported that vibrations worsened the fuel cell performance. Even though recent studies seem to be more representative of real-world vibration and with more developed characterisation techniques, the results regarding the effects of vibration are still inconclusive. Further experimental investigations could include: i) implementation of in-situ water visualisation techniques to assess the effects of vibration, either detrimental or beneficial, on the fuel cell performance and ii) ex-situ investigations on the degradation of the fuel cell components (e.g. SEM imaging, synchrotron X-ray) to further explain the evolution in performance caused by the changes in the electro-physical properties of the fuel cell components. Thus far, to the authors' knowledge, protection means of the fuel cell under vibration have not been reported in literature. At least, no academic publication was found on the topic. Therefore, future studies on the effects of vibration on fuel cell performance should include vibration protection systems for fuel cells.

2.3. Freeze/thaw cycles

According to the US Department of Energy (DoE) technical targets for fuel cell power systems [94], fuel cells must be able to start and operate at environmental conditions at which ambient temperature may drop below 0 °C. Working at such subfreezing temperatures leads to ice formation. As it is well known, as water freezes, its volume expands. This expansion creates uneven stresses within the fuel cell stack that may damage the fuel cell components (e.g. GDL broken fibres, cracks, delamination and Pt particle migration [95]). In addition, as water thaws, its volume diminishes and the created stresses vanish. These Freeze/Thaw (F/T) cycles may damage the fuel cell components and lead to a decrease in the fuel cell performance. The effects of subfreezing conditions, on either the fuel cell performance or its individual

components, have already been covered in literature [95–100]. Hou et al. [99] employed the EIS technique to investigate the effects of residual water on a PEFC operating at repetitive sub-zero conditions (-10 °C). It was reported that the ohmic resistance remains unchanged after eight freezing cycles regardless of the amount of residual water. In contrast, mass transport resistance was shown to be highly dependent on the amount of residual water. In line with [99], Alink et al. [96] investigated the effects of subfreezing operating conditions (varying between -40°C and 100°C) on both the PEFC performance and the physical properties of its components. In this study, the performance of two stacks with different initial states (dry and wet) was investigated. It was shown that after repeated F/T cycles (62 F/T and 120 F/T cycles for wet and dry state, respectively), only a small performance degradation was witnessed for the fuel cell with an initial dry state, especially at high current densities, whereas the fuel cell with a wet initial state showed major performance degradation. This was explained by less efficient water management; resulting in more prominent flooding effects. Moreover, a decrease in the electrocatalyst surface area (ECSA) and an increase in porosity were observed for both stacks. These effects were more marked for the F/T cycles applied to the stack with a wet initial state.

Alink et al. [96] reported that only a small water content freezes inside the membrane whereas most of the water freezes in the electrodes causing cavities and micro-cracks. The authors concluded that removing water from the cell before freezing is helpful to mitigate performance degradation caused by repeated F/T cycles. The authors also reported that compression of GDLs and MEAs restrains the formation of severe cracks and electrode material detachment. Furthermore, designing the fuel cell components with more flexible materials would tolerate volume expansion caused by ice formation and thus prevent physical damage of the stack components caused by the induced stresses. This proposition is in good agreement with the results reported by Lee et al. [100] where MEAs were prepared in-house by distributing catalyst ink over the electrolyte. By comparing commercial MEAs with some in-house prepared ones, the latter showed no significant structural changes caused by the water/ice formation. This was

attributed to the good membrane-CL interfacial properties resulting from directly spraying the catalyst ink onto the membrane. The authors concluded that the F/T degradation is caused by the initial component microstructure, which is in turn related to the process of fabrication of the fuel cell components.

Guo and Qi [97] investigated the effect of F/T cycles (between -30°C and 20°C) on the physical properties of the MEA. For a fully hydrated membrane, physical damage in the CL was observed, namely catalyst domain segregation and cracks, in conjunction with a loss in the ECSA. Moreover, the authors reported that the volume expansion created by water freezing may induce considerable stress in the assembled PEFCs. The report concluded that lowering the water content in the membrane could mitigate the MEA damage caused by F/T cycles. Lee et al. [98] studied the effect of MPL on the PEFC degradation caused by F/T cycles (between -15°C and 70°C). The authors compared the performance degradation in an MPL-coated GDL and in an uncoated one. For both GDLs, the performance degradation was observed as the number of F/T cycles was increased. The authors reported that the MPL-coated GDL showed an earlier degradation in the CL compared to the uncoated one. This was attributed to the fact that when the fuel cell operation is stopped, using a MPL keeps more water in the membrane and the CL. This leads to ice formation and thus volume expansion, which may in turn lead to a compression induced stresses. From EIS analysis, it was shown that a MPL-coated GDL delays the performance degradation caused by the mass transport resistance and maintains it at a lower value compared to the uncoated GDL.

Gavello et al. [95] examined the effects of repetitive freezing conditions on a single cell PEFC. SEM images analysis showed a limited number of broken fibres, cracks and delamination areas, which may be attributed to the induced mechanical stress caused by the formation and thawing of ice within the fuel cell components. Furthermore, a strong migration of Pt particles from the CL to the membrane was observed, which could be a reason for the performance degradation due to the ice formation within the MEA. This finding is in contrast with the results of [96] where it was reported that due to ice formation, few Pt particles detach from the CL,

pass through the GDL, and are finally transported via the exhaust gases. Thus, further investigations of this issue need to be carried out.

From the reported studies, it was proven that the degradation related to F/T cycles is caused by water volume expansion, decrease in the ECSA, and Pt particles migration. However, no study has reported the induced compression value caused by operating the fuel cell at subfreezing conditions. Knowing such a value would be of major importance to help modellers to accurately predict the F/T-induced stresses.

2.4. Hygrothermal-induced stresses

Fuel cells are subjected to external and internal temperature variations, which may lead to the development of expansion forces within the fuel cell components. Heat management is of paramount importance for PEFCs since they repel roughly 50 to 70% of chemical energy contained in the hydrogen in form of heat [101]. Internal heat generation may come from different processes: i) the ohmic resistance losses, ii) entropic heat of reactions, and iii) irreversible heat of electrochemical reactions [102]. These heat generation processes present approximately 10%, 55%, and 35% of the overall amount of the released heat, respectively [102]. Fuel cells are also subjected to temperature variations from their external environments, with portable and transportation fuel cell applications more likely to be operated at temperatures ranging from higher to sub-zero levels. These temperature variations add up to the induced stresses within the fuel cell and depend on the different thermal expansion coefficients of the fuel cell components and the fuel cell assembly system.

Khandelwal and Mench [103] measured the thermal through-plane conductivity and contact resistance of different fuel cell components. The authors reported that the thermal conductivity of the GDL decreases with increasing temperature. This latter may have detrimental effects as the GDLs play an important role in conducting temperature from the membrane and CLs to the BPPs that have means for heat removal. Correlation between GDL compression and thermal

contact resistance was also emphasised by the authors in [103]. It was reported that the thermal contact resistance between the GDL and an aluminium bronze material dropped from 6.7×10^{-4} to 2.0×10^{-4} m^2KW^{-1} as the compression increased from 0.4 to 2.2 MPa. Cui et al. [104] reported a study on the degradation of polymer gaskets used in PEFCs. In this study, liquid silicone rubber (LSR) was investigated as a sealing gasket material. It was shown that during the temperature change, the thermal contraction and expansion of the LSR cause nearly all of the stress variation. In addition, the temperature history was shown to have important correlation with the stiffness variation of the LSR material. In another study, Lai et al. [105] investigated the effects of cycling on the mechanical properties of a Nafion® NR-111 membrane. Among several results, the authors reported crack formation caused by the resulting stress as the membrane was subjected to in-situ cycling experiments between dry and wet conditions. The induced cracks led to gas crossover and thus fuel cell performance degradation. This effect was shown to be less pronounced as the membrane was subjected to shorter humidity fluctuations.

With regard to the stresses caused by the hydration state of the membrane, Mason et al. [106] reported some important compression and thickness changes caused by the MEA hydration. It was shown that flooding conditions increase the membrane hydration resulting in an increase of the stress across the MEA. The authors concluded that the generated stresses from repetitive hydration cycles, e.g. due to start-up and shutdown procedures, could lead to long-term degradation of the fuel cell performance. In line with [106], de la Cruz et al. [17] reported an increase of 22% of the weight of a fully hydrated MEA compared to a dry one. This was explained in terms of water retention of the membrane. It was also reported that excess water could expand the membrane by 10%-15% in all directions [17]. Given that the membrane is constrained by the adjacent fuel cell components, the membrane expansion leads to the appearance of a creeping effect in the areas beneath the channels. This expansion is presumed to push the GDL inside the channels and could lead to mechanical failures of the

membrane. The authors also reported that the constrained membranes showed a reduced water uptake, which may have detrimental effect on its ionic conductivity.

Generated stresses caused by the membrane swelling received important attention in the literature. However, no experimental mechanical measures of these stresses have been reported so far. Quantifying these stresses might be of major importance especially for model development. In contrast, little has been done concerning the temperature induced stresses of the other cell components. This might be due to the negligible thermal expansion of materials caused by either internal or external temperature variations.

Table 1 highlights relevant conclusions regarding the effects of mechanical stresses on the PEFC components properties.

Mechanical stress sources	**Effects on components properties**	**Ref.**
Clamping pressure	GDL carbon fibre crushing.	[44]
	Reduction in the porosity of the GDL.	[44,48,50,55]
	Reduction in the electrical contact resistance between the cell components (generally between the GDL and the BPP).	[8,43,44,52–54]
	GDL protrusion into the BPPs' channels.	[42,44,48]
	Reduction in the water management capacity.	[50]
	Increase in the mass transport resistance.	[8,43,52,53]
	High stress regions located at the edges compared to the centre of the GDL (point-load assembly design).	[15–18,60]
	Decrease in the GDL's thermal contact resistance.	[103]

Vibration	Unchanged electrical contact resistance.	[76]
	Increase in the hydrogen leakage rate.	[77,81]
	Increase in the ohmic resistance (electronic, ionic and contact resistance).	[78,80,81]
	Decrease in the hydrogen use.	[79]
	Decrease in the stack electrical insulation.	[77]
	Improvement in the excess liquid water evacuation.	[85–90]
Freeze/thaw cycles	Unchanged ohmic resistance	[99]
	Reduction in the electrocatalyst surface area (ECSA).	[96,97]
	Increase in the porosity of the electrode.	[96]
	Appearance of cavities and micro-cracks on the electrodes.	[95–97]
	Migration of Pt particles from the CL to the membrane.	[95]
	Migration of Pt particles from the CL to the exhaust gases.	[96]
Hygrothermal-induced stresses	Decrease in the thermal conductivity of the GDL upon increasing temperature.	[103]
	Membrane crack formation caused by cycling experiments between dry and wet conditions.	[105]

Table 1. Relevant conclusions regarding the effects of mechanical stresses on the PEFC components properties.

As shown in this section, various compression mechanisms take place in operating PEFCs and may affect their performances. In order to understand these effects, especially on the GDL, the following section aims to give an overview of the intrinsic characteristics of the GDL that

may affect its electro-physical characteristics with respect to the applied mechanical compression.

3. Effects of mechanical compression on the GDL characteristics

The electro-physical properties of the GDL are highly influenced by the mechanical compression, as the GDL was reported to be the component most subjected to structural deformation under mechanical compression [43]. As a result, the effects of mechanical compression on this component's properties were already investigated in the literature. Thus far, different aspects were investigated by researchers focusing on the in-situ investigations of the effects of mechanical compression on GDL properties. Under this section, the effects of mechanical compression on the following GDL characteristics are reported: MPL coating, PTFE loading, and the induced effects on the water management within the GDL.

3.1. MPL coating

The GDL substrate is often coated with a microporous layer (MPL) either on one side, which is generally the catalyst layer side, or on both sides of the GDL, the so-called double-side MPL coating [107]. The MPL is fabricated from carbon particles and hydrophobic agent (typically PTFE). Coating GDLs with MPL aims to improve the GDL electro-physical characteristics by reducing the contact resistance and by enhancing the water transport and removal capacity of PEFCs [9–11]. MPL also improves the membrane humidification as it enhances its water retention by keeping water within the membrane.

Sadeghifar [36] studied the effect of MPL coating on the GDL electrical conductivity. Among several findings, it was shown that the MPL coating significantly decreases the electrical

conductivity of the MPL-coated GDLs since the MPL electrical conductivity is much lower than the GDL's one (conductivity of carbon black is lower in comparison with carbon fibres [36]). The difference between the GDL and the MPL conductivities was seen to increase upon increasing compression. This latter was attributed to the fact that GDL conductivity increases with increasing compression whereas MPL conductivity reaches a plateau at high compression. It was also shown that MPL coating significantly increases the contact resistance between the GDL and the BPP. In contrast with [36], Ismail et al. [20] measured the electrical contact resistance as a function of the clamping pressure for both uncoated (Sigracet® 10BA) and MPL-coated GDLs (Sigracet® 10BC and 10BE). The electrical contact resistance was shown to be lower for the MPL-coated GDLs compared to the uncoated GDL. These findings were explained by the presence of more conductive carbon particles in the MPL compared to the GDL substrate. The reduction in the contact resistance between the MPL-coated GDLs and the BPP was also attributed to the compressible nature of the MPLs that favour them to occupy the gaps that exist in the surface of the BPPs and thus enlargens the surface contact between the BPP and the GDL.

Regarding the effect of MPL coating on fuel cells operating in real life conditions and under different compressive loads, Dotelli et al. [8] investigated the effect of compression on three carbon cloth GDLs. Two of the GDL substrates were coated by MPL. The compression ratio of the cell, i.e. the ratio of the operating thickness of the GDL to its original thickness, was set at either 30% or 50%. The ohmic resistance was shown to decrease in the uncoated GDL upon increasing compression ratio whereas it stayed unchanged in the other two MPL coated GDLs. At a compression ratio of 50%, the uncoated GDL showed the worst performance compared to the other MPL-coated GDLs. In addition, the MPL-coated GDLs showed higher power density compared to the uncoated one as the reduction in the mass transport resistance (due to the MPL coating) had more pronounced effect on the performance than the reduction in the ohmic resistance.

3.2. GDL hydrophobic content

The GDL is typically treated with PTFE to improve its water repellent characteristics. However, the PTFE conductivity was reported to be several times lower than that of the carbon fibres [36]. This low conductivity may affect the overall electrical conductivity of the PTFE-treated GDLs. Ismail et al. [20] measured the in-plane electrical conductivity of a number of untreated and PTFE-treated GDLs. The authors reported that the in-plane conductivity remains almost unchanged regardless of the PTFE loading. This was explained by the structure of carbon fibres that remains unaffected upon adding PTFE particles. The through-plane resistance was shown to increase with increasing PTFE content; this was attributed to the electrically insulating nature of the PTFE particles. These findings agree well with [36]. PTFE loading was also reported to affect the thermal conductivity of the GDLs. A decrease by a factor of two in the through-plane thermal conductivity was reported by Khandelwal and Mench [103] from their measurements of treated (20wt% PTFE) and untreated GDLs.

Tötzke et al. [108] conducted a study on the influence of hydrophobic treatment on the structure of compressed GDLs (Freudenberg H2315 with different PTFE loadings). It was reported that PTFE loading reduces the GDL penetration into the gas channels by improving the stiffness of the GDL substrate and enhancing the shape of the GDL as smoother surfaces of PTFE-treated GDLs, compared to untreated ones, were witnessed when the mechanical compression was applied. This latter might be beneficial to mitigate water management issues since the protruded fibre endings in the case of untreated GDLs (Figure 7 (A)) could form potential barrier for water droplets removal and thus lead to water accumulation in the gas channels. Figure 7 (D) depicts the effect of PTFE loading on the GDL penetration into the gas channels with respect to the applied compression. It can be seen that PTFE loading decreases the penetration depth leading to less deformation of the investigated GDLs. Comparable protrusion behaviour of T20A and T10A was attributed to similar PTFE loading on the upper regions of the GDLs used.

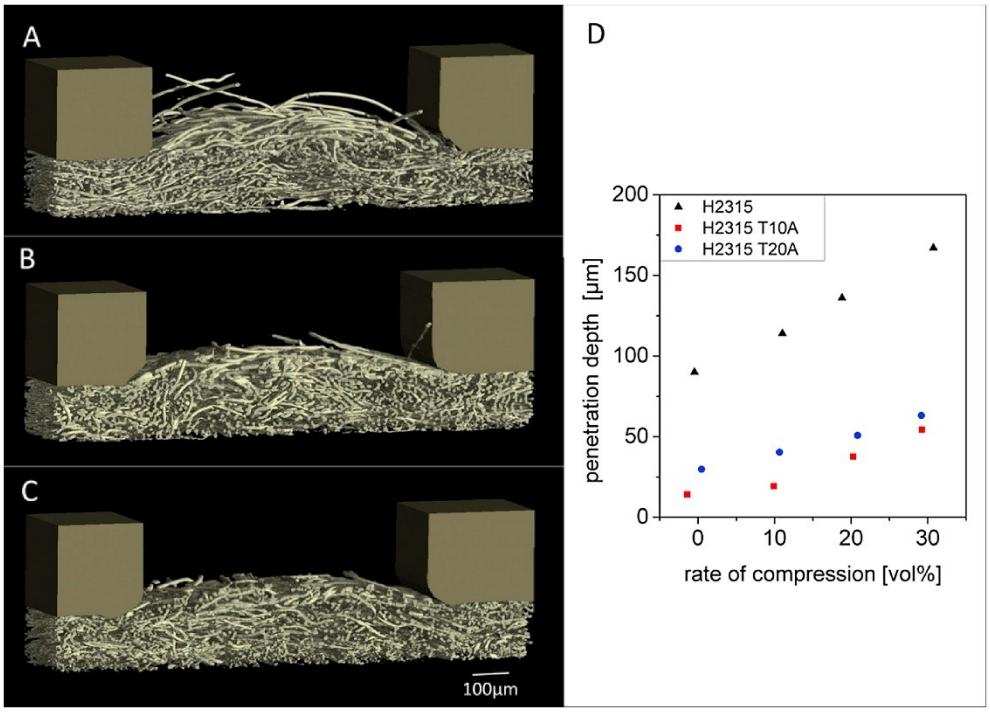

Figure 7. *3D-view of the compressed sample at a compression ratio of 30%: (A) H2315 (0 wt% PTFE); (B) H2315 T10A (10 wt% PTFE); (C) H2315 T20A (20 wt% PTFE). (D) GDL penetration into the gas channel as a function of the applied compression. From [108].*

Dotelli et al. [8] studied the effect of MPL's PTFE loading on the fuel cell performance with respect to the applied mechanical compression, by comparing two MPLs with different PTFE contents (40% and 12%) and under different compression ratios (30% and 50%). The results obtained from the analysis of power and polarisation curves showed that the effect of PTFE content within the MPL has a minor impact on the fuel cell performance. However, this impact became more noticeable at high current densities where the MPL with high hydrophobic content (40% PTFE) showed better performance compared to the MPL with low hydrophobic content (12% PTFE). These results were attributed to the fact that high PTFE content results in higher hydrophobicity, which helps to evacuate the excess water produced at the cathode CL at high current densities. The authors concluded that MPL hydrophobicity improves the fuel cell performance by reducing the mass transport resistance at high current densities. In line with [8], Ferreira et al. [109] reported that MEAs with PTFE-treated GDLs showed a better

performance than the ones with untreated GDLs. This was attributed to the fact that GDL hydrophobic treatment provided an enhanced overall water management inside the fuel cell.

In a recent study carried out by Biesdorf et al. [110], the authors investigated the effects of the hydrophobic coating on the mass transport resistance in an operating PEFC. GDLs were subjected to a 25% compression ratio. It was found that among different PTFE loadings, the cell with the highest amount of PTFE showed the lowest amount of water accumulation; in contrast, high mass transport losses were detected in fuel cells with high PTFE content. Hence, it was concluded that high mass transport losses are not always associated with higher amount of water accumulation. This was explained by different morphologies of water accumulation. Namely, in hydrophobic GDLs, water accumulates in form of droplets leading to restricted areas for reactants transport. In GDLs with lower PTFE content, water accumulates in form of films, allowing more paths for reactant gases to reach the CL. Water management within the GDL will be addressed in more details in the following section.

In summary, the electro-physical characteristics of GDLs have a major impact on the performance of the fuel cell when it is subjected to mechanical stresses. Two main factors were analysed, namely the MPL coating and the PTFE loading, as these factors present a considerable part of the reported studies in the literature so far. Correlations between GDL characteristics and PEFC performance with regard to the applied mechanical stresses have been reported in the literature [37,64,65]. Nevertheless, future studies combining both in-situ and ex-situ characterisation techniques could investigate the effects of the variation in the electrophysical properties of the GDL on the PEFC performance as a function of the applied mechanical compression. The objective of such studies could be the research of the relationship between in-situ and ex-situ observed performance of the GDL component.

Table 2. highlights relevant conclusions regarding the effects of the MPL coating and hydrophobic content treatments on the GDL electro-physical characteristics.

GDL treatments	Effects on the GDL electro-physical characteristics	Ref.
MPL coating	Reduction in the electrical conductivity of the MPL-coated GDLs. Increase in the electrical contact resistance between the GDL and the BPP.	[36]
	Reduction in the mass transport resistance of the MPL-coated GDLs.	[8]
	Larger surface contact between the BPP and the GDL. Reduction in the electrical contact resistance between the GDL and the BPP.	[20]
	Stagnation of MPL-coated GDLs' electrical resistance upon increasing mechanical compression.	[20,36]
Hydrophobic agent	Unchanging GDL's electrical in-plane conductivity regardless of the PTFE loading.	[20]
	Increase in the electrical through-plane resistance with increasing PTFE content.	[20,36]
	Increase in the mass transport resistance with high PTFE content.	[110]
	Reduction in the GDL penetration into the gas channels by improving the stiffness of the GDL substrate.	[108]
	Reduction in the mass transport resistance at high current densities due to the improved water evacuation.	[8,109]
	Decrease in the GDL's through-plane thermal conductivity.	[103]

Table 2. Summary of relevant conclusions regarding the effects of the MPL coating and hydrophobic content on the GDL electro-physical characteristics.

3.3. Water management

PEFC water management has been widely covered in the literature due to its strong association with fuel cell performance. In order to ensure a good ionic conductivity of the electrolyte, the membrane (perfluorosulfonic acid, PFSA) needs to be well hydrated. Hence, water might be provided through the anode and/or cathode stream gases to hydrate the electrolyte, at least for stacks with power levels higher than 1 kW. However, excess water may cause electrode flooding. The latter occurs when the rate of liquid water accumulation outpaces the rate of water removal. Under these conditions, GDL pores get clogged and reactant gases do not reach the CLs leading to an increase in mass transport losses and therefore to a decrease in fuel cell performance caused by reactant starvation. These effects are more pronounced when mechanical compression is applied leading to a decrease in the porosity of GDL [111].

Liquid water is more apparent at the cathode side where it is generated as a product of the cell reaction on the cathode CL. Moreover, the transport of hydrogen protons through the membrane accompanies the transport of water molecules from the anode to the cathode side in a phenomenon commonly referred to as electroosmotic drag [112,113]. The latter also increases the water content at the cathode side. In addition, the electroosmotic drag and the water production at the cathode side create a concentration gradient that leads to the transport of a portion of water from the cathode to the anode side via back diffusion through the membrane [113,114]. The water transport mechanisms in PEFCs have been comprehensively reviewed in [112]. The accumulated water at the cathode of a PEFC is generally removed from the fuel cell via the gas stream at the cathode flow channels [112]. Besides the fact that water accumulation may cause flooding, the protonic conductivity of PFSA membranes was reported to be highly dependent on its water uptake [115]. Therefore, a dynamic balance of water is needed in order to achieve an effective water removal along with a proper hydration state of the membrane [112].

Cha et al. [116] carried out a study on the effects of assembly pressure on both the PEFC performance and its water management using EIS technique. Their apparatus consisted of a single cell with a Toray TGP-H-120 GDL. The compression process was carried out through varying the clamping torque on the bolts of the fuel cell assembly. It was shown that the ohmic resistance decreased as the clamping torque increased, which was attributed to the decrease in the contact resistance and also the increase in the membrane hydration on the anode side. The latter was explained by the decrease in the porosity and the permeability of the GDL as the assembly pressure increased leading to a higher back-diffusion water transport mechanism (from the cathode to the anode side) and therefore a uniform membrane hydration. It was also seen that as the current density increased, the ohmic resistance decreased, which was reported to be due to better membrane hydration caused by the increase in water generation on the cathode side. However, excessive compression was reported to increase the mass transport resistance that was attributed to water accumulation on the cathode side leading to flooding conditions. The report concluded that the fuel cell assembly pressure needs to be optimised in agreement with the water content in the PEFC.

Mason et al. [106] investigated the effects of flooding on the dimensional changes of the MEA. They reported that as flooding occurred, the membrane thickness increased leading to the appearance of higher stresses, which in turn had detrimental effects on the GDL (e.g. carbon fibres crushing). The report concluded that flooding effects might lead to long-term fuel cell performance degradation. In this regard, development of in-situ water visualisation techniques plays a major role in the assessment of water management capacity of the PEFCs. Various visualisation techniques have been reported in the literature, e.g. neutron imaging, X-ray microtomography, electron microscopy, and fluorescence microscopy. For more details on the water visualisation techniques, the reader shall be referred to the review study reported by Bazylak [117]. Even though numerous studies have been conducted on the water management issue, little has been done on the effect of mechanical compression on water management in operating PEFCs. Bazylak et al. [118] reported a study on the effect of

compression on liquid water management. The authors used an ex-situ apparatus allowing visualisation of liquid water based on fluorescence microscopy. The GDL used (Toray TGP-H-060) was placed under an optically transparent clamping plate with a clamping pressure of 1.5 MPa. The authors reported that the compressed regions of the GDL present preferential pathways for water transport and break-through. This finding, which is in contrast to the expected behaviour of the water transport within the GDL, was reported to be due to the loss of hydrophobicity in the compressed regions of the GDL. In the study reported by Bazylak et al. [118], SEM images showed that compression causes carbon fibres and PTFE coating breakage, which was reported to lead to the degradation of the hydrophobic content in the compressed regions. This, in turn, favours the water accumulation in the regions beneath the ribs compared to the regions beneath the channels where the hydrophobic agents are less impacted by compression. The authors in [118] concluded that the reported water transport behaviour might be beneficial for PEFC performance since the liquid water can be located in the GDL regions under the ribs where water accumulation is less critical than the regions under the channels (e.g possible creation of diffusion barriers leading to reactants starvation). Similar results were also reported in a study carried out by Ince et al. [119]. The authors experimentally investigated the water distribution using thermographic and synchrotron X-ray imaging. They employed a water injection point method where liquid water was injected directly beneath the MPL before reaching the GDL substrate. Two GDL samples were investigated in this study: i) Sigracet® 29BC with a compression ratio of 11%, and ii) Sigracet® 25BC with a compression ratio of 21%, referred to as the uncompressed and the compressed GDL sample, respectively. It was observed that the pore saturation of the compressed GDL was higher than the one of the uncompressed GDL in both the MPL and the GDL substrate. Furthermore, water transport in the in-plane direction of the compressed GDL was higher compared to the uncompressed GDL. These results indicate that compression promotes in-plane water transport in the compressed regions of the GDL.

Zenyuk et al. [120] employed the X-ray computed thermography technique to investigate water distribution in GDLs with different compression ratios of 15%, 35%, and 47%. The GDL used was a carbon paper Sigracet® 10BA. The authors reported that the porosity of the GDLs is higher under the channels compared to the porosity under the ribs. In contrast to the results reported in [118,121], liquid water was shown to flow through the higher porosity pathways, indicating that areas beneath the channels present preferential pathways for water transport within the GDL. Moreover, it was shown that as the compression increases, the size of water agglomeration decreases and form small clusters located mostly underneath the channels. The study concluded that future improvements of fuel cell design might include GDLs with modulated porosity, which will enhance water removal capacity by directing liquid water through desired porosity pathways.

With regard to in-situ water visualisation studies, Manke et al. [122] investigated the water transport and evolution in an operating PEFC by means of high-resolution synchrotron X-ray radiography. It was shown that liquid water clusters are located in the areas beneath the channels in an operating PEFC. Hartnig et al. [121] carried out a study on the transport of liquid water in operating PEFCs using high-resolution synchrotron X-ray radiography. Their test apparatus consisted of a single channel PEFC with a Sigracet® 10BB GDL. Figure 8 shows the through plane observation of initial spots of liquid water. It can be seen that liquid water clusters under the ribs are higher compared to the ones under the channels, which is in good agreement with the ex-situ results reported in [118].

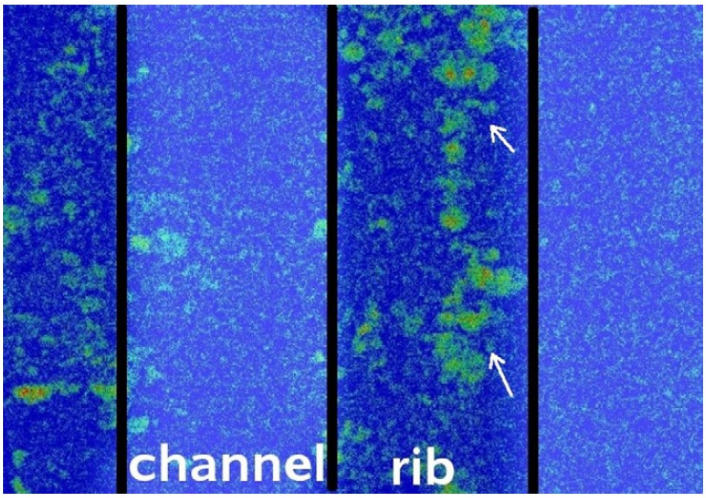

Figure 8. *Spots of liquid water accumulation beneath the rib of the BPP (bright spots). From [121].*

Water management is one of the major issues affecting the cell's mechanical behaviour and electrical performance. In order to investigate the effect of mechanical compression on water management, in-situ and ex-situ characterisation techniques, with more focus on the latter, have been employed by a number of research teams worldwide. Many authors reported some causal relationships between water management issues and the applied mechanical compression. Preferential pathways for water transport in the GDLs under mechanical compression are still a subject of debate, some studies reported that water is preferentially transported in the compressed regions underneath the ribs [118,121] whereas others claimed preferential pathways in the areas beneath the channels [120]. Therefore, the results regarding this subject are still inconclusive. Moreover, although a number of in-situ water visualisation techniques exist, as have been employed by different authors using synchrotron X-ray radiography [121,122] and neutron imaging [123–125], to the authors' knowledge, the use of these techniques to conduct specific investigations about the effects of mechanical compression on water management in an operating PEFC is still limited. The use of such techniques would be of major importance in order to validate some previous assumptions regarding the impacts of mechanical compression on the water management capacity of operating PEFCs [126].

4. Synthesis of the literature review

Table 3 summarises the previously reported studies with regard to the effects of mechanical compression on both the fuel cell performance and the components properties by way of in-situ electrochemical and mechanical characterisation techniques.

Used technique	Investigation	Compression method	Compression measurement	Active area (cm^2)	Single cell / stack	GDL Type	GDL initial thickness (µm)	GDL initial thickness measurement	Membrane / MEA used	Pt loading	FPP	Compression range MPa	Other compression data	Year of study	Ref
Polarisation curves Pressure sensitive films	-Effect of stack clamping pressure -Optimal clamping torque determination with regard to the GDL type	Clamping torque on four bolts	Pressure sensitive films	10	Single cell	Toray, ELAT, and CARBEL series 100 combined with Toray	Toray: 203, ELAT:508, and CARBEL series 100 combined with Toray :279	Measured at nine points on the GDL surface	Gore ™ PRIMEA® Series 5000	0.3 mg cm^{-2} for both anode and cathode	Serpentine flow channels	Toray: 1.61, 1.8, and 2.08 MPa ELAT: 8.37, 9.3, and > 9.35 MPa CARBEL – Toray:7.34, 8.6, and 8.75 MPa	Clamping torque of 11.3, 14.12, and 16.94 N.m	1999	[45]
Polarisation curves	-Effect of GDL compression on the PEFC performance	Clamping torque on eight bolts plus a large central screw	Two gauges on the both cell sides	50	Single cell	ELAT carbon cloth with a double sided MPL Toray carbon fibre paper with a MPL	N/A	N/A	Nafion® 115	0.4 mg cm^{-2} for both anode and cathode	Single serpentine flow channels	N/A	Compression ratios[2] ranging from 10% to 45%	2006	[49]
Polarisation curves Measurement of electro-physical properties of the GDL	-Effect of stack clamping pressure -Optimal clamping torque determination	N/A	N/A	25	Single cell	Toray	120	Measured with a thickness gauge	N/A	N/A	Serpentine graphite of five uniformly spaced	Clamping pressure of 0.2, 1, and 2 MPa	N/A	2007	[37]

											channels and bends				
Polarisation curves Pressure sensitive films	-Effect of stack clamping pressure -Pressure distribution analysis	Compression unit using torque wrench on central bolt pushing a flat metal plate	Clamping torque from torque wrench	25	Single cell	Toray H-060	N/A	N/A	N/A	3.5 mg m^{-3}	Single serpentine with ribs and channels width of 1.5 mm.	Clamping pressure from 0.8 to 5 MPa	N/A	2007	[55]
Polarisation curves Electrical conductivity, gas permeability measurements SEM images	-Effect of GDL compression and material properties	N/A	N/A	25	Single cell	Carbon fibre cloth OC14 and NC14	OC14: 510 NC14: 430	N/A	Nafion® NRE212	N/A	Serpentine graphite plate	N/A	Compression ratios ranging from 3% to 90%.	2008	[38]
Polarisation curves Pressure sensitive films	-Effects of clamping torque and bolt configuration -Pressure distribution analysis	2, 4, and 6 clamping blots torque (according to USFCC[1])	Clamping torque from torque wrench Post-processing of pressure sensitive films' images	100	Single & 10 cell stack	Toray carbon paper (TGP-H-090)	N/A	N/A	Nafion® 212	Anode and cathode Pt/Ru 0.5 mg cm^{-2} and Pt 0.65 mg cm^{-2},respectively	Pelcan® graphite BPP, 155 x 85 x4 mm, three-parallel-channel serpentine flow fields, cathode and anode channel width 1 and	N/A	Clamping torque values of 8, 12, and 16 Nm	2009	[18]

											0.6 mm, respectively				
Piezoresistive pressure sensitive film	-Assembly pressure distribution	Torque bolts	Directly from a calibrated torque wrench	50	Single cell	N/A	N/A	N/A	N/A	N/A	N/A	N/A	Torque bolts of 2, 4, 6, 8, 10, and 11 Nm	2009	[15]
Polarisation curves	-Effect of stack clamping pressure -Performance stability under anode reformate gas condition	Clamping torque on six bolts	N/A	N/A	5 cell stack	Sigracet® 10BC carbon-fibre felt with MPL	380	Manufacturer data from SGL	Gore ™ PRIMEA® series 57	N/A	N/A	N/A	Compression ratios of 15% and 30%	2010	[54]
Polarisation curves EIS analysis	-Effect of endplate thickness (through numerical simulations) and bolt torques (experimental)	Clamping torque on six bolts	N/A	225	Single & 50 cell stack	N/A	N/A	N/A	N/A	N/A	Graphite plates	N/A	Clamping torque ranging from 5 to 30 Nm	2010	[52]
Polarisation curves EIS analysis	-Effect of clamping pressure uniformity and clamping torque -Optimal clamping torque determination	Clamping torque on six bolts	N/A	225	Single & three cell stack	MPL coated Sigracet® carbon cloth	N/A	N/A	Nafion® 112	0.4 mg cm^{-2} for both anode and cathode	Parallel serpentine	N/A	Clamping torque ranging from 5 to 30 Nm	2010	[53]
Polarisation curves Piezoresistive pressure sensitive film	-Effect of bolt torques and gasket materials -Pressure distribution analysis	Clamping torque on four bolts	N/A	25	Single cell	Textron Carbon cloth GDL	350	Measured with a thickness gauge	Nafion® 115	0.1 mg cm^{-2} for both anode and cathode	Graphite plates	N/A	Clamping torque ranging from 7 to 13 Nm	2011	[16]

Polarisation and power curves measurements EIS analysis SEM images	-Effect of GDL compression and MPL coating	Clamping torque	N/A	25	Single cell	MPL coated and uncoated carbon cloth (SAATI SpA)	-MPL Coated GDLs: ~420 - 450 -Uncoated GDL : ~400	Measured from SEM images	Nafion® 212	0.3 mg cm^{-2} at the anode and 0.6 mg cm^{-2} for the cathode	Anode: Single serpentine Cathode: triple parallel serpentine	N/A	Compression ratios of 30 and 50 %	2011	[8]
EIS analysis Dimensional change analysis Electrolyte membrane resistance measurement	-Effect of membrane hydration and electrodes flooding on the dimensional change and the PEFC performance	Controlled Compression Unit (CCU)	Directly from the CCU	5	Single cell	Toray H-060	N/A	N/A	Nafion® 117	N/A	Single serpentine with land and channel width of 1.2 mm and 1.1 mm respectively .	Clamping pressure from 0.2 to 1.2 MPa	N/A	2013	[106]
Polarisation curves EIS analysis Dimensional change analysis	-Effect of assembly pressure	Cell Compression Unit (CCU)	Directly from the CCU	5	Single cell	Toray H-060	190	Manufacturer data From Toray	Nafion® 212	N/A	Single serpentine with land and channel width of 1.2 mm and 1.1 mm respectively .	Clamping pressure from 0.5 to 2.5 MPa	N/A	2013	[43]
Pressure sensitive films	-Effects of :clamping pressure, clamping duration, central	Torque wrench on the bolts and hydraulic press	Clamping torque from torque wrench	N/A	16 cell stack	- MPL coated GDL	- MPL Coated GDL: 254	Measured using a digital caliper	N/A	N/A	N/A	Ranging from 0.5 to 2.5 MPa with an	Clamping torque: 10.17 N.m	2013	[60]

	compressive load, and GDL type	on the centre region of the stack				- uncoated GDL	- Uncoated GDL: 140					increment of 0.5 MPa	Hydraulic press: 59.16 N, 11.12 kN, 15.57 kN		
Polarisation curves EIS analysis SEM images Electrical resistivity measurement Capillary flow porometry	-Effect of compressive loads on the pore structure of the GDLs -Determination of optimal clamping pressure and pore structure	GDLs compressed ex-situ using a hydraulic press	Pressures from the hydraulic press	6.25	Single cell	Carbon cloth GDL	N/A	N/A	Nafion® 212	0.9 mg cm^{-2} (total) for both anode and cathode	N/A	19.61, 58,8, and 98 MPa	Compression ratios of 16.6, 22.2, and 30.55%	2014	[50]
Polarisation curves EIS analysis	-Effect of assembly pressure on PEFC performance and water management	Clamping torque	N/A	25	Single cell	Toray TGP-H-120	N/A	N/A	Gore ™ M815 series	N/A	Three lines modified serpentine with ribs and channels width of 1.2 mm.	N/A	Clamping torque ranging from 5.9 to 8.9 Nm	2015	[116]
Pressure distribution analysis Polarisation curves	-Optimal clamping torque determination	Clamping torque on eight bolts	N/A	20	Single cell	N/A	N/A	N/A	Nafion® 212	0.6 mg cm^{-2} for both anode and cathode	Graphite, double serpentine flow channels for anode and parallel flow channels for cathode	0.5 to 3 MPa (only for ex-situ measurement of the contact resistance)	Clamping torque values 0.5, 1.0, 1.5, 2.0, and 2.5 Nm	2016	[57]

Polarisation curves EIS analysis Pressure sensitive films SEM images	-Effect of GDL compression on oxygen transport -Pressure distribution analysis	Clamping torque on eight bolts	Calculated from the measured variation in the thickness of the gaskets	5	Single cell	MPL coated GDL: Sigracet 25BC Uncoated GDL: Sigracet 25BA	25BC: 220 ± 10 24BA: 153 ± 14	Measured with a thickness gauge and SEM images	Gore ™ A510.1/M 715.18/C5 80.4	0.1 mg cm^{-2} at the anode and 0.4 mg cm^{-2} for the cathode	Serpentine graphite plates with ribs and channels width of 0.5 mm.	N/A	Compression ratios ranging from 8 to 53%	2017	[111]

Table 3. Summary of literature studies on the effects of mechanical compression on PEFC performance.

[1]United State Fuel Cell Council

[2]The ratio of the operating thickness of the GDL to its original thickness

5. Conclusion and future prospects

Through the application of in-situ characterisation techniques, valuable information regarding the effects of mechanical compression on the performance of operating PEFCs has been widely reported in the literature. In this regard, a literature-based analysis has been carried out in order to give a comprehensive overview on the previously reported studies on the effects of mechanical compression and their respective impacts on the fuel cell performance and component properties. First, both internal and external mechanical compression mechanisms along with their respective impacts were presented. Then, the effects of mechanical compression on GDL properties and its water management were analysed. Finally, a summary of the studies focusing on the in-situ characterisation of the effect of mechanical compression on PEFC performance by way of electrochemical and mechanical techniques was provided. From this literature review, the following conclusions can be drawn:

- The development of new compression methods, devices, and materials, allowing homogeneous pressure distribution and dissipating the pressure concentration on the edges of the PEFC components, is needed to mitigate the detrimental impacts of mechanical compression on the PEFC performance.
- Although extended studies have been conducted on water management and in-situ liquid water visualisation techniques, dedicated investigations on the effect of mechanical compression by the use of in-situ water visualisation technique are still needed in the literature. Using such techniques would help for either validating or disapproving various hypothesis and conclusions reported in the literature. Thus, proper implementation of in-situ water visualisation techniques in mechanical

compression studies is needed for further investigations on the effects of mechanical compression on the water management in PEFCs.

- Both pressure sensitive and piezo-resistive films have been used to assess the generated mechanical stresses under the assembly pressure. However, these techniques allow the investigation of pressure distribution in off-line fuel cells (i.e. not in operation). Therefore, reports on new techniques that allow measuring the generated stresses during PEFC operations are lacking in the literature, e.g. smart composite structures with embedded mechanical stress measurement devices. The development of such new tools would be of major benefit for the understanding of stresses generated during PEFC operations and it could be of major help for the development of enhanced PEFC multi-physical models.
- Real-world vibration tests were carried out on PEFCs mounted on either vibrating platforms or on real vehicles. However, the investigated fuel cells were usually not in operation during vibration and the performance tests were carried out on steady test benches either after vibration tests or at regular periods during tests. It would be interesting to investigate the effects of real-world vibration on the fuel cell performance using real-time procedures. The use of such characterisation procedures would help to assess the variations of the PEFC performance while undergoing real-world vibration conditions, which is more representative of the real-life operating PEFCs.
- Freeze/thaw cycles related performance degradation was attributed to the water volume expansion and Pt particles migration. However, no study has measured the induced compression value caused by freezing conditions so far. Knowing such values would be of major importance to help modellers to accurately determine the F/T-induced stresses.
- Various researchers have investigated the issue of optimal PEFC assembly pressure. Yet, in most of the cases, incohesive clamping parameters were used, e.g. cell compression procedures, cell operating conditions, single cell, fuel cell stacks, and components. Therefore, this lack of cohesion makes difficult, if not impossible, to draw

a conclusion concerning the optimal assembly pressure. Moreover, the research of optimal clamping pressure was only related to the performance of the fuel cell without considering the clamping process, therefore, studies combining both clamping mechanisms and optimal clamping pressure are lacking in the literature. In order to optimise the PEFC performance, future investigations may include the research of both optimal clamping pressure and its adequate clamping mechanism as a function of the final application of the fuel cell since the mechanical stresses may differ from one application to another (e.g. stationary, portable, and transportation).

- With regard to the pressure distribution across the fuel cell stack components, it has been well recognised that, for a typical fuel cell assembly method (namely point-load designs with bolts and nuts), the pressure distribution concentrates on the edges of the fuel cell components whereas the centre receives much lower clamping load. In order to reduce this inhomogeneity, new techniques allowing the mitigation of the effects related to this issue have already been reported in the patent literature. However, no comparative studies have been carried out to investigate these techniques even though it may have a major impact towards the enhancement of fuel cell performance. Thus, it would be interesting for future studies to investigate the advantages and drawbacks of different compression retention systems reported in the patent literature.
- Although some studies have combined both in-situ and ex-situ characterisation techniques in order to investigate the effects of mechanical compression, causal relationships between in-situ and ex-situ observed performance are still needed in the literature. Therefore, there is still a large area to explore in order to deepen our understanding of the effect of mechanical compression on the PEFCs performance through combining both in-situ and ex-situ characterisation techniques.

Acknowledgments

The “Région Bourgogne-Franche-Comté” is gratefully acknowledged for its support through the ELICOP Project (Ref. 2015C-4944 and 2015-4948) and the co-funding of KHETABI El Mahdi’s PhD thesis (Convention N° 2017 Y_07529). In addition, the authors would like to gratefully acknowledge the Plastic Omnium company for the support given to this research project.

References

[1] P.P. Edwards, V.L. Kuznetsov, W.I.F. David, N.P. Brandon, Hydrogen and fuel cells: Towards a sustainable energy future, Energy Policy. 36 (2008) 4356–4362. doi:10.1016/j.enpol.2008.09.036.

[2] J. Andrews, B. Shabani, Re-envisioning the role of hydrogen in a sustainable energy economy, International Journal of Hydrogen Energy. 37 (2012) 1184–1203. doi:10.1016/j.ijhydene.2011.09.137.

[3] M. Chahartaghi, B.A. Kharkeshi, Performance analysis of a combined cooling, heating and power system with PEM fuel cell as a prime mover, Applied Thermal Engineering. 128 (2018) 805–817. doi:10.1016/j.applthermaleng.2017.09.072.

[4] M. Gandiglio, A. Lanzini, M. Santarelli, P. Leone, Design and optimization of a proton exchange membrane fuel cell CHP system for residential use, Energy and Buildings. 69 (2014) 381–393. doi:10.1016/j.enbuild.2013.11.022.

[5] X. Chen, G. Gong, Z. Wan, L. Luo, J. Wan, Performance analysis of 5 kW PEMFC-based residential micro-CCHP with absorption chiller, International Journal of Hydrogen Energy. 40 (2015) 10647–10657. doi:10.1016/j.ijhydene.2015.06.139.

[6] C. Kalyvas, A. Kucernak, D. Brett, G. Hinds, S. Atkins, N. Brandon, Spatially resolved diagnostic methods for polymer electrolyte fuel cells: a review, Wiley Interdisciplinary Reviews: Energy and Environment. 3 (2014) 254–275. doi:10.1002/wene.86.

[7] L. Holzer, O. Pecho, J. Schumacher, P. Marmet, O. Stenzel, F.N. Büchi, A. Lamibrac, B. Münch, Microstructure-property relationships in a gas diffusion layer (GDL) for Polymer Electrolyte Fuel Cells, Part I: effect of compression and anisotropy of dry GDL, Electrochimica Acta. 227 (2017) 419–434. doi:10.1016/j.electacta.2017.01.030.

[8] G. Dotelli, L. Omati, P. Gallo Stampino, P. Grassini, D. Brivio, Investigation of gas diffusion layer compression by electrochemical impedance spectroscopy on running polymer electrolyte membrane fuel cells, Journal of Power Sources. 196 (2011) 8955–8966. doi:10.1016/j.jpowsour.2011.01.078.

[9] Z. Qi, A. Kaufman, Improvement of water management by a microporous sublayer for PEM fuel cells, Journal of Power Sources. 109 (2002) 38–46. doi:10.1016/S0378-7753(02)00058-7.

[10] J.H. Nam, K.-J. Lee, G.-S. Hwang, C.-J. Kim, M. Kaviany, Microporous layer for water morphology control in PEMFC, International Journal of Heat and Mass Transfer. 52 (2009) 2779–2791. doi:10.1016/j.ijheatmasstransfer.2009.01.002.

[11] Z. Lu, M.M. Daino, C. Rath, S.G. Kandlikar, Water management studies in PEM fuel cells, part III: Dynamic breakthrough and intermittent drainage characteristics from GDLs with and without MPLs, International Journal of Hydrogen Energy. 35 (2010) 4222–4233. doi:10.1016/j.ijhydene.2010.01.012.

[12] A. El-kharouf, T.J. Mason, D.J.L. Brett, B.G. Pollet, Ex-situ characterisation of gas diffusion layers for proton exchange membrane fuel cells, Journal of Power Sources. 218 (2012) 393–404. doi:10.1016/j.jpowsour.2012.06.099.
[13] Y. Zhou, G. Lin, A.J. Shih, S.J. Hu, Multiphysics Modeling of Assembly Pressure Effects on Proton Exchange Membrane Fuel Cell Performance, J. Fuel Cell Sci. Technol. 6 (2009) 041005-041005-7. doi:10.1115/1.3081426.
[14] S.-J. Lee, C.-D. Hsu, C.-H. Huang, Analyses of the fuel cell stack assembly pressure, Journal of Power Sources. 145 (2005) 353–361. doi:10.1016/j.jpowsour.2005.02.057.
[15] R. Montanini, G. Squadrito, G. Giacoppo, EXPERIMENTAL EVALUATION OF THE CLAMPING PRESSURE DISTRIBUTION IN A PEM FUEL CELL USING MATRIX-BASED PIEZORESISTIVE THIN-FILM SENSORS, (2009) 6.
[16] I. Gatto, F. Urbani, G. Giacoppo, O. Barbera, E. Passalacqua, Influence of the bolt torque on PEFC performance with different gasket materials, International Journal of Hydrogen Energy. 36 (2011) 13043–13050. doi:10.1016/j.ijhydene.2011.07.066.
[17] J. de la Cruz, U. Cano, T. Romero, Simulation and in situ measurement of stress distribution in a polymer electrolyte membrane fuel cell stack, Journal of Power Sources. 329 (2016) 273–280. doi:10.1016/j.jpowsour.2016.08.073.
[18] C.-Y. Wen, Y.-S. Lin, C.-H. Lu, Experimental study of clamping effects on the performances of a single proton exchange membrane fuel cell and a 10-cell stack, Journal of Power Sources. 192 (2009) 475–485. doi:10.1016/j.jpowsour.2009.03.058.
[19] J.H. Chun, K.T. Park, D.H. Jo, S.G. Kim, S.H. Kim, Numerical modeling and experimental study of the influence of GDL properties on performance in a PEMFC, International Journal of Hydrogen Energy. 36 (2011) 1837–1845. doi:10.1016/j.ijhydene.2010.01.036.
[20] M.S. Ismail, T. Damjanovic, D.B. Ingham, M. Pourkashanian, A. Westwood, Effect of polytetrafluoroethylene-treatment and microporous layer-coating on the electrical conductivity of gas diffusion layers used in proton exchange membrane fuel cells, Journal of Power Sources. 195 (2010) 2700–2708. doi:10.1016/j.jpowsour.2009.11.069.
[21] C. Lim, C.Y. Wang, Effects of hydrophobic polymer content in GDL on power performance of a PEM fuel cell, Electrochimica Acta. 49 (2004) 4149–4156. doi:10.1016/j.electacta.2004.04.009.
[22] C.S. Kong, D.-Y. Kim, H.-K. Lee, Y.-G. Shul, T.-H. Lee, Influence of pore-size distribution of diffusion layer on mass-transport problems of proton exchange membrane fuel cells, Journal of Power Sources. 108 (2002) 185–191. doi:10.1016/S0378-7753(02)00028-9.
[23] Y. Bultel, K. Wiezell, F. Jaouen, P. Ozil, G. Lindbergh, Investigation of mass transport in gas diffusion layer at the air cathode of a PEMFC, Electrochimica Acta. 51 (2005) 474–488. doi:10.1016/j.electacta.2005.05.007.
[24] S. Park, B.N. Popov, Effect of cathode GDL characteristics on mass transport in PEM fuel cells, Fuel. 88 (2009) 2068–2073. doi:10.1016/j.fuel.2009.06.020.
[25] D. Liu, S. Case, Durability study of proton exchange membrane fuel cells under dynamic testing conditions with cyclic current profile, Journal of Power Sources. 162 (2006) 521–531. doi:10.1016/j.jpowsour.2006.07.007.
[26] S. Zhang, X. Yuan, H. Wang, W. Mérida, H. Zhu, J. Shen, S. Wu, J. Zhang, A review of accelerated stress tests of MEA durability in PEM fuel cells, International Journal of Hydrogen Energy. 34 (2009) 388–404. doi:10.1016/j.ijhydene.2008.10.012.
[27] B. Wahdame, D. Candusso, F. Harel, X. François, M.-C. Péra, D. Hissel, J.-M. Kauffmann, Analysis of a PEMFC durability test under low humidity conditions and stack behaviour modelling using experimental design techniques, Journal of Power Sources. 182 (2008) 429–440. doi:10.1016/j.jpowsour.2007.12.122.
[28] K. Tüber, D. Pócza, C. Hebling, Visualization of water buildup in the cathode of a transparent PEM fuel cell, Journal of Power Sources. 124 (2003) 403–414. doi:10.1016/S0378-7753(03)00797-3.
[29] R. Satija, D.L. Jacobson, M. Arif, S.A. Werner, In situ neutron imaging technique for evaluation of water management systems in operating PEM fuel cells, Journal of Power Sources. 129 (2004) 238–245. doi:10.1016/j.jpowsour.2003.11.068.

[30] D. Spernjak, A.K. Prasad, S.G. Advani, Experimental investigation of liquid water formation and transport in a transparent single-serpentine PEM fuel cell, Journal of Power Sources. 170 (2007) 334–344. doi:10.1016/j.jpowsour.2007.04.020.
[31] J. Wu, X.Z. Yuan, H. Wang, M. Blanco, J.J. Martin, J. Zhang, Diagnostic tools in PEM fuel cell research: Part I Electrochemical techniques, International Journal of Hydrogen Energy. 33 (2008) 1735–1746. doi:10.1016/j.ijhydene.2008.01.013.
[32] A. Arvay, E. Yli-Rantala, C.-H. Liu, X.-H. Peng, P. Koski, L. Cindrella, P. Kauranen, P.M. Wilde, A.M. Kannan, Characterization techniques for gas diffusion layers for proton exchange membrane fuel cells – A review, Journal of Power Sources. 213 (2012) 317–337. doi:10.1016/j.jpowsour.2012.04.026.
[33] S. El Oualid, R. Lachat, D. Candusso, Y. Meyer, Characterization process to measure the electrical contact resistance of Gas Diffusion Layers under mechanical static compressive loads, International Journal of Hydrogen Energy. 42 (2017) 23920–23931. doi:10.1016/j.ijhydene.2017.03.130.
[34] H. Sadeghifar, N. Djilali, M. Bahrami, Thermal conductivity of a graphite bipolar plate (BPP) and its thermal contact resistance with fuel cell gas diffusion layers: Effect of compression, PTFE, micro porous layer (MPL), BPP out-of-flatness and cyclic load, Journal of Power Sources. 273 (2015) 96–104. doi:10.1016/j.jpowsour.2014.09.062.
[35] S. Prass, S. Hasanpour, P.K. Sow, A.B. Phillion, W. Mérida, Microscale X-ray tomographic investigation of the interfacial morphology between the catalyst and micro porous layers in proton exchange membrane fuel cells, Journal of Power Sources. 319 (2016) 82–89. doi:10.1016/j.jpowsour.2016.04.031.
[36] H. Sadeghifar, In-plane and through-plane electrical conductivities and contact resistances of a Mercedes-Benz catalyst-coated membrane, gas diffusion and micro-porous layers and a Ballard graphite bipolar plate: Impact of humidity, compressive load and polytetrafluoroethylene, Energy Conversion and Management. 154 (2017) 191–202. doi:10.1016/j.enconman.2017.10.060.
[37] W.R. Chang, J.J. Hwang, F.B. Weng, S.H. Chan, Effect of clamping pressure on the performance of a PEM fuel cell, Journal of Power Sources. 166 (2007) 149–154. doi:10.1016/j.jpowsour.2007.01.015.
[38] J.-H. Lin, W.-H. Chen, Y.-J. Su, T.-H. Ko, Effect of gas diffusion layer compression on the performance in a proton exchange membrane fuel cell, Fuel. 87 (2008) 2420–2424. doi:10.1016/j.fuel.2008.03.001.
[39] J. Millichamp, T.J. Mason, T.P. Neville, N. Rajalakshmi, R. Jervis, P.R. Shearing, D.J.L. Brett, Mechanisms and effects of mechanical compression and dimensional change in polymer electrolyte fuel cells – A review, Journal of Power Sources. 284 (2015) 305–320. doi:10.1016/j.jpowsour.2015.02.111.
[40] A.M. Dafalla, F. Jiang, Stresses and their impacts on proton exchange membrane fuel cells: A review, International Journal of Hydrogen Energy. 43 (2018) 2327–2348. doi:10.1016/j.ijhydene.2017.12.033.
[41] W. Zhang, C. Wu, Effect of Clamping Load on the Performance of Proton Exchange Membrane Fuel Cell Stack and Its Optimization Design: A Review of Modeling and Experimental Research, J. Fuel Cell Sci. Technol. 11 (2013) 020801-020801-11. doi:10.1115/1.4026070.
[42] S.G. Kandlikar, Z. Lu, T.Y. Lin, D. Cooke, M. Daino, Uneven gas diffusion layer intrusion in gas channel arrays of proton exchange membrane fuel cell and its effects on flow distribution, Journal of Power Sources. 194 (2009) 328–337. doi:10.1016/j.jpowsour.2009.05.019.
[43] T.J. Mason, J. Millichamp, P.R. Shearing, D.J.L. Brett, A study of the effect of compression on the performance of polymer electrolyte fuel cells using electrochemical impedance spectroscopy and dimensional change analysis, International Journal of Hydrogen Energy. 38 (2013) 7414–7422. doi:10.1016/j.ijhydene.2013.04.021.
[44] T.J. Mason, J. Millichamp, T.P. Neville, A. El-kharouf, B.G. Pollet, D.J.L. Brett, Effect of clamping pressure on ohmic resistance and compression of gas diffusion layers for polymer

electrolyte fuel cells, Journal of Power Sources. 219 (2012) 52–59. doi:10.1016/j.jpowsour.2012.07.021.
[45] W. Lee, C.-H. Ho, J.W. Van Zee, M. Murthy, The effects of compression and gas diffusion layers on the performance of a PEM fuel cell, Journal of Power Sources. 84 (1999) 45–51. doi:10.1016/S0378-7753(99)00298-0.
[46] I. Nitta, T. Hottinen, O. Himanen, M. Mikkola, Inhomogeneous compression of PEMFC gas diffusion layer: Part I. Experimental, Journal of Power Sources. 171 (2007) 26–36. doi:10.1016/j.jpowsour.2006.11.018.
[47] P.H. Chi, S.H. Chan, F.B. Weng, A. Su, P.C. Sui, N. Djilali, On the effects of non-uniform property distribution due to compression in the gas diffusion layer of a PEMFC, International Journal of Hydrogen Energy. 35 (2010) 2936–2948. doi:10.1016/j.ijhydene.2009.05.066.
[48] N. Khajeh-Hosseini-Dalasm, T. Sasabe, T. Tokumasu, U. Pasaogullari, Effects of polytetrafluoroethylene treatment and compression on gas diffusion layer microstructure using high-resolution X-ray computed tomography, Journal of Power Sources. 266 (2014) 213–221. doi:10.1016/j.jpowsour.2014.05.004.
[49] J. Ge, A. Higier, H. Liu, Effect of gas diffusion layer compression on PEM fuel cell performance, Journal of Power Sources. 159 (2006) 922–927. doi:10.1016/j.jpowsour.2005.11.069.
[50] V. Senthil Velan, G. Velayutham, N. Rajalakshmi, K.S. Dhathathreyan, Influence of compressive stress on the pore structure of carbon cloth based gas diffusion layer investigated by capillary flow porometry, International Journal of Hydrogen Energy. 39 (2014) 1752–1759. doi:10.1016/j.ijhydene.2013.11.038.
[51] L.P. Wang, L.H. Zhang, J.P. Jiang, Experimental Study of Assembly Clamping Pressure on Performance of PEM Fuel Cells, Applied Mechanics and Materials. (2011). doi:10.4028/www.scientific.net/AMM.44-47.2399.
[52] S. Asghari, M.H. Shahsamandi, M.R. Ashraf Khorasani, Design and manufacturing of end plates of a 5kW PEM fuel cell, International Journal of Hydrogen Energy. 35 (2010) 9291–9297. doi:10.1016/j.ijhydene.2010.02.135.
[53] S. Asghari, A. Mokmeli, M. Samavati, Study of PEM fuel cell performance by electrochemical impedance spectroscopy, International Journal of Hydrogen Energy. 35 (2010) 9283–9290. doi:10.1016/j.ijhydene.2010.03.069.
[54] S.-D. Yim, B.-J. Kim, Y.-J. Sohn, Y.-G. Yoon, G.-G. Park, W.-Y. Lee, C.-S. Kim, Y.C. Kim, The influence of stack clamping pressure on the performance of PEM fuel cell stack, Current Applied Physics. 10 (2010) S59–S61. doi:10.1016/j.cap.2009.11.042.
[55] T. Ous, C. Arcoumanis, Effect of compressive force on the performance of a proton exchange membrane fuel cell, Proceedings of the Institution of Mechanical Engineers, Part C: Journal of Mechanical Engineering Science. 221 (2007) 1067–1074. doi:10.1243/09544062JMES654.
[56] H.M. Chang, M.H. Chang, Effects of Assembly Pressure on the Gas Diffusion Layer and Performance of a PEM Fuel Cell, Applied Mechanics and Materials. (2012). doi:10.4028/www.scientific.net/AMM.110-116.48.
[57] N.U. Hassan, M. Kilic, E. Okumus, B. Tunaboylu, A.M. Soydan, Experimental determination of optimal clamping torque for AB-PEM fuel cell, Journal of Electrochemical Science and Engineering. 6 (2016) 9–16. doi:10.5599/jese.198.
[58] C. Carral, N. Charvin, H. Trouvé, P. Mélé, An experimental analysis of PEMFC stack assembly using strain gage sensors, International Journal of Hydrogen Energy. 39 (2014) 4493–4501. doi:10.1016/j.ijhydene.2014.01.033.
[59] Prescale | Fujifilm Global, (n.d.). http://www.fujifilm.com/products/prescale/prescalefilm/ (accessed July 4, 2018).
[60] A. Bates, S. Mukherjee, S. Hwang, S.C. Lee, O. Kwon, G.H. Choi, S. Park, Simulation and experimental analysis of the clamping pressure distribution in a PEM fuel cell stack, International Journal of Hydrogen Energy. 38 (2013) 6481–6493. doi:10.1016/j.ijhydene.2013.03.049.

[61] M.K. Debe, Electrocatalyst approaches and challenges for automotive fuel cells, Nature. 486 (2012) 43–51. doi:10.1038/nature11115.
[62] H. Sadeghifar, N. Djilali, M. Bahrami, Effect of Polytetrafluoroethylene (PTFE) and micro porous layer (MPL) on thermal conductivity of fuel cell gas diffusion layers: Modeling and experiments, Journal of Power Sources. 248 (2014) 632–641. doi:10.1016/j.jpowsour.2013.09.136.
[63] Pressure Mapping Sensor 5076, Tekscan. (n.d.). https://www.tekscan.com/products-solutions/pressure-mapping-sensors/5076 (accessed July 6, 2018).
[64] A. El-Kharouf, N.V. Rees, R. Steinberger-Wilckens, Gas Diffusion Layer Materials and their Effect on Polymer Electrolyte Fuel Cell Performance – Ex Situ and In Situ Characterization, Fuel Cells. 14 (2014) 735–741. doi:10.1002/fuce.201300247.
[65] A. El-kharouf, R. Steinberger-Wilckens, The Effect of Clamping Pressure on Gas Diffusion Layer Performance in Polymer Electrolyte Fuel Cells, Fuel Cells. 15 (2015) 802–812. doi:10.1002/fuce.201500088.
[66] T.D. Bogumil, E.J. Connor, A.G. Chinnici, P.F. Spacher, M.W. Keyser, Side spring compression retention system, US8012648B2, 2011. https://patents.google.com/patent/US8012648B2/en (accessed August 11, 2018).
[67] B. Andreas-Schott, G.W. Fly, J.A. Rock, I.R. Jermy, Fuel cell stack compression retention system with external springs, US7807316B2, 2010. https://patents.google.com/patent/US7807316/en (accessed August 11, 2018).
[68] B. Andreas-Schott, A. Chinnici, Y.-H. Lai, G.W. Fly, Fuel cell compression retention system using compliant strapping, US20080305380A1, 2008. https://patents.google.com/patent/US20080305380A1/en (accessed August 11, 2018).
[69] B. Andreas-Schott, J.A. Rock, G.W. Fly, T.P. Migliore, Fuel cell stack compression retention system using overlapping sheets, US20080311457A1, 2008. https://patents.google.com/patent/US20080311457A1/en (accessed August 11, 2018).
[70] S.J. Imen, M. Shakeri, Vibration Modeling of PEM Fuel Cell for Prediction of Cell Number Effects by Experimental Data, Fuel Cells. 16 (2016) 193–204. doi:10.1002/fuce.201500206.
[71] G.R. Watts, V.V. Krylov, Ground-borne vibration generated by vehicles crossing road humps and speed control cushions, Applied Acoustics. 59 (2000) 221–236. doi:10.1016/S0003-682X(99)00026-2.
[72] V. Rouss, P. Lesage, S. Bégot, D. Candusso, W. Charon, F. Harel, X. François, V. Selinger, C. Schilo, S. Yde-Andersen, Mechanical behaviour of a fuel cell stack under vibrating conditions linked to aircraft applications part I: Experimental, International Journal of Hydrogen Energy. 33 (2008) 6755–6765. doi:10.1016/j.ijhydene.2008.08.032.
[73] G. Diloyan, M. Sobel, K. Das, P. Hutapea, Effect of mechanical vibration on platinum particle agglomeration and growth in Polymer Electrolyte Membrane Fuel Cell catalyst layers, Journal of Power Sources. 214 (2012) 59–67. doi:10.1016/j.jpowsour.2012.04.027.
[74] S.H. El-Emam, A.A. Mousa, M.M. Awad, Effects of stack orientation and vibration on the performance of PEM fuel cell, International Journal of Energy Research. 39 (2015) 75–83. doi:10.1002/er.3217.
[75] S.J. Imen, M. Shakeri, Reliability Evaluation of an Open-Cathode PEMFC at Operating State and Longtime Vibration by Mechanical Loads, Fuel Cells. 16 (2016) 126–134. doi:10.1002/fuce.201500144.
[76] N. Rajalakshmi, S. Pandian, K.S. Dhathathreyan, Vibration tests on a PEM fuel cell stack usable in transportation application, International Journal of Hydrogen Energy. 34 (2009) 3833–3837. doi:10.1016/j.ijhydene.2009.03.002.
[77] Y. Hou, W. Zhou, C. Shen, Experimental investigation of gas-tightness and electrical insulation of fuel cell stack under strengthened road vibrating conditions, International Journal of Hydrogen Energy. 36 (2011) 13763–13768. doi:10.1016/j.ijhydene.2011.07.092.
[78] Y. Hou, B. Zhou, W. Zhou, C. Shen, Y. He, An investigation of characteristic parameter variations of the polarization curve of a proton exchange membrane fuel cell stack under

strengthened road vibrating conditions, International Journal of Hydrogen Energy. 37 (2012) 11887–11893. doi:10.1016/j.ijhydene.2012.05.030.
[79] Y. Hou, D. Hao, C. Shen, Z. Shao, Experimental investigation of the steady-state efficiency of fuel cell stack under strengthened road vibrating condition, International Journal of Hydrogen Energy. 38 (2013) 3767–3772. doi:10.1016/j.ijhydene.2013.01.037.
[80] Y. Hou, X. Zhang, X. Lu, D. Hao, L. Ma, P. Li, AC impedance characteristics of a vehicle PEM fuel cell stack under strengthened road vibrating conditions, International Journal of Hydrogen Energy. 39 (2014) 18362–18368. doi:10.1016/j.ijhydene.2014.09.054.
[81] Y. Hou, D. Hao, J. Shen, P. Li, T. Zhang, H. Wang, Effect of strengthened road vibration on performance degradation of PEM fuel cell stack, International Journal of Hydrogen Energy. 41 (2016) 5123–5134. doi:10.1016/j.ijhydene.2016.01.072.
[82] A. Haji Hosseinloo, M.M. Ehteshami, Shock and vibration effects on performance reliability and mechanical integrity of proton exchange membrane fuel cells: A critical review and discussion, Journal of Power Sources. 364 (2017) 367–373. doi:10.1016/j.jpowsour.2017.08.037.
[83] M.C. Bétournay, G. Bonnell, E. Edwardson, D. Paktunc, A. Kaufman, A.T. Lomma, The effects of mine conditions on the performance of a PEM fuel cell, Journal of Power Sources. 134 (2004) 80–87. doi:10.1016/j.jpowsour.2004.02.026.
[84] X. Wang, S. Wang, S. Chen, T. Zhu, X. Xie, Z. Mao, Dynamic response of proton exchange membrane fuel cell under mechanical vibration, International Journal of Hydrogen Energy. 41 (2016) 16287–16295. doi:10.1016/j.ijhydene.2016.06.082.
[85] V. Palan, W.S. Shepard, Enhanced water removal in a fuel cell stack by droplet atomization using structural and acoustic excitation, Journal of Power Sources. 159 (2006) 1061–1070. doi:10.1016/j.jpowsour.2005.12.020.
[86] V. Palan, W.S. Shepard, K.A. Williams, Removal of excess product water in a PEM fuel cell stack by vibrational and acoustical methods, Journal of Power Sources. 161 (2006) 1116–1125. doi:10.1016/j.jpowsour.2006.06.021.
[87] H.K. Ma, S.H. Huang, Y.Z. Kuo, A novel ribbed cathode polar plate design in piezoelectric proton exchange membrane fuel cells, Journal of Power Sources. 185 (2008) 1154–1161. doi:10.1016/j.jpowsour.2008.07.019.
[88] H.-K. Ma, S.-H. Huang, J.-S. Wang, C.-G. Hou, C.-C. Yu, B.-R. Chen, Experimental study of a novel piezoelectric proton exchange membrane fuel cell with nozzle and diffuser, Journal of Power Sources. 195 (2010) 1393–1400. doi:10.1016/j.jpowsour.2009.09.033.
[89] H.-K. Ma, J.-S. Wang, Y.-T. Chang, Development of a novel pseudo bipolar piezoelectric proton exchange membrane fuel cell with nozzle and diffuser, Journal of Power Sources. 196 (2011) 3766–3772. doi:10.1016/j.jpowsour.2010.12.093.
[90] H.K. Ma, H.M. Cheng, W.Y. Cheng, F.M. Fang, W.F. Luo, Development of a piezoelectric proton exchange membrane fuel cell stack (PZT-Stack), Journal of Power Sources. 240 (2013) 314–322. doi:10.1016/j.jpowsour.2013.03.161.
[91] N. Bussayajarn, H. Ming, K.K. Hoong, W.Y. Ming Stephen, C.S. Hwa, Planar air breathing PEMFC with self-humidifying MEA and open cathode geometry design for portable applications, International Journal of Hydrogen Energy. 34 (2009) 7761–7767. doi:10.1016/j.ijhydene.2009.07.077.
[92] D.T. Santa Rosa, D.G. Pinto, V.S. Silva, R.A. Silva, C.M. Rangel, High performance PEMFC stack with open-cathode at ambient pressure and temperature conditions, International Journal of Hydrogen Energy. 32 (2007) 4350–4357. doi:10.1016/j.ijhydene.2007.05.042.
[93] S.U. Jeong, E.A. Cho, H.-J. Kim, T.-H. Lim, I.-H. Oh, S.H. Kim, Effects of cathode open area and relative humidity on the performance of air-breathing polymer electrolyte membrane fuel cells, Journal of Power Sources. 158 (2006) 348–353. doi:10.1016/j.jpowsour.2005.09.044.
[94] Fuel Cell Technologies Office Multi-Year Research, Development, and Demonstration Plan | Department of Energy, (2016). https://www.energy.gov/eere/fuelcells/downloads/fuel-cell-technologies-office-multi-year-research-development-and-22 (accessed July 6, 2018).

[95] G. Gavello, J. Zeng, C. Francia, U.A. Icardi, A. Graizzaro, S. Specchia, Experimental studies on Nafion® 112 single PEM-FCs exposed to freezing conditions, International Journal of Hydrogen Energy. 36 (2011) 8070–8081. doi:10.1016/j.ijhydene.2011.01.182.
[96] R. Alink, D. Gerteisen, M. Oszcipok, Degradation effects in polymer electrolyte membrane fuel cell stacks by sub-zero operation—An in situ and ex situ analysis, Journal of Power Sources. 182 (2008) 175–187. doi:10.1016/j.jpowsour.2008.03.074.
[97] Q. Guo, Z. Qi, Effect of freeze-thaw cycles on the properties and performance of membrane-electrode assemblies, Journal of Power Sources. 160 (2006) 1269–1274. doi:10.1016/j.jpowsour.2006.02.093.
[98] Y. Lee, B. Kim, Y. Kim, X. Li, Effects of a microporous layer on the performance degradation of proton exchange membrane fuel cells through repetitive freezing, Journal of Power Sources. 196 (2011) 1940–1947. doi:10.1016/j.jpowsour.2010.10.028.
[99] J. Hou, W. Song, H. Yu, Y. Fu, Z. Shao, B. Yi, Electrochemical impedance investigation of proton exchange membrane fuel cells experienced subzero temperature, Journal of Power Sources. 171 (2007) 610–616. doi:10.1016/j.jpowsour.2007.07.015.
[100] S.-Y. Lee, H.-J. Kim, E. Cho, K.-S. Lee, T.-H. Lim, I.C. Hwang, J.H. Jang, Performance degradation and microstructure changes in freeze–thaw cycling for PEMFC MEAs with various initial microstructures, International Journal of Hydrogen Energy. 35 (2010) 12888–12896. doi:10.1016/j.ijhydene.2010.08.070.
[101] M.R. Islam, B. Shabani, G. Rosengarten, J. Andrews, The potential of using nanofluids in PEM fuel cell cooling systems: A review, Renewable and Sustainable Energy Reviews. 48 (2015) 523–539. doi:10.1016/j.rser.2015.04.018.
[102] H. Ju, H. Meng, C.-Y. Wang, A single-phase, non-isothermal model for PEM fuel cells, International Journal of Heat and Mass Transfer. 48 (2005) 1303–1315. doi:10.1016/j.ijheatmasstransfer.2004.10.004.
[103] M. Khandelwal, M.M. Mench, Direct measurement of through-plane thermal conductivity and contact resistance in fuel cell materials, Journal of Power Sources. 161 (2006) 1106–1115. doi:10.1016/j.jpowsour.2006.06.092.
[104] T. Cui, Y.J. Chao, J.W.V. Zee, C.-H. Chien, Effect of Temperature on Mechanical Property Degradation of Polymeric Materials, in: Challenges in Mechanics of Time-Dependent Materials, Volume 2, Springer, Cham, 2015: pp. 41–47. doi:10.1007/978-3-319-06980-7_5.
[105] Y.-H. Lai, C.K. Mittelsteadt, C.S. Gittleman, D.A. Dillard, Viscoelastic Stress Analysis of Constrained Proton Exchange Membranes Under Humidity Cycling, J. Fuel Cell Sci. Technol. 6 (2009) 021002-021002-13. doi:10.1115/1.2971045.
[106] T.J. Mason, J. Millichamp, T.P. Neville, P.R. Shearing, S. Simons, D.J.L. Brett, A study of the effect of water management and electrode flooding on the dimensional change of polymer electrolyte fuel cells, Journal of Power Sources. 242 (2013) 70–77. doi:10.1016/j.jpowsour.2013.05.045.
[107] G.-M. Huang, M.-H. Chang, Effect of Gas Diffusion Layer With Double-Side Microporous Layer Coating on Proton Exchange Membrane Fuel Cell Performance Under Different Air Inlet Relative Humidity, Int. J. Electrochem. Sci. 9 (2014) 13.
[108] C. Tötzke, G. Gaiselmann, M. Osenberg, T. Arlt, H. Markötter, A. Hilger, A. Kupsch, B.R. Müller, V. Schmidt, W. Lehnert, I. Manke, Influence of hydrophobic treatment on the structure of compressed gas diffusion layers, Journal of Power Sources. 324 (2016) 625–636. doi:10.1016/j.jpowsour.2016.05.118.
[109] R.B. Ferreira, D.S. Falcão, V.B. Oliveira, A.M.F.R. Pinto, Experimental study on the membrane electrode assembly of a proton exchange membrane fuel cell: effects of microporous layer, membrane thickness and gas diffusion layer hydrophobic treatment, Electrochimica Acta. 224 (2017) 337–345. doi:10.1016/j.electacta.2016.12.074.
[110] J. Biesdorf, A. Forner-Cuenca, T.J. Schmidt, P. Boillat, Impact of Hydrophobic Coating on Mass Transport Losses in PEFCs, J. Electrochem. Soc. 162 (2015) F1243–F1252. doi:10.1149/2.0861510jes.

[111] C. Simon, F. Hasché, H.A. Gasteiger, Influence of the Gas Diffusion Layer Compression on the Oxygen Transport in PEM Fuel Cells at High Water Saturation Levels, J. Electrochem. Soc. 164 (2017) F591–F599. doi:10.1149/2.0691706jes.
[112] K. Jiao, X. Li, Water transport in polymer electrolyte membrane fuel cells, Progress in Energy and Combustion Science. 37 (2011) 221–291. doi:10.1016/j.pecs.2010.06.002.
[113] F. Barbir, PEM Fuel Cells, Second Edition: Theory and Practice, 2 edition, Academic Press, Amsterdam, 2012.
[114] A. Iranzo, P. Boillat, Liquid water distribution patterns featuring back-diffusion transport in a PEM fuel cell with neutron imaging, International Journal of Hydrogen Energy. 39 (2014) 17240–17245. doi:10.1016/j.ijhydene.2014.08.042.
[115] T.A. Zawodzinski, T.E. Springer, J. Davey, R. Jestel, C. Lopez, J. Valerio, S. Gottesfeld, A Comparative Study of Water Uptake By and Transport Through Ionomeric Fuel Cell Membranes, J. Electrochem. Soc. 140 (1993) 1981–1985. doi:10.1149/1.2220749.
[116] D. Cha, J.H. Ahn, H.S. Kim, Y. Kim, Effects of clamping force on the water transport and performance of a PEM (proton electrolyte membrane) fuel cell with relative humidity and current density, Energy. 93 (2015) 1338–1344. doi:10.1016/j.energy.2015.10.045.
[117] A. Bazylak, Liquid water visualization in PEM fuel cells: A review, International Journal of Hydrogen Energy. 34 (2009) 3845–3857. doi:10.1016/j.ijhydene.2009.02.084.
[118] A. Bazylak, D. Sinton, Z.-S. Liu, N. Djilali, Effect of compression on liquid water transport and microstructure of PEMFC gas diffusion layers, Journal of Power Sources. 163 (2007) 784–792. doi:10.1016/j.jpowsour.2006.09.045.
[119] U.U. Ince, H. Markötter, M.G. George, H. Liu, N. Ge, J. Lee, S.S. Alrwashdeh, R. Zeis, M. Messerschmidt, J. Scholta, A. Bazylak, I. Manke, Effects of compression on water distribution in gas diffusion layer materials of PEMFC in a point injection device by means of synchrotron X-ray imaging, International Journal of Hydrogen Energy. 43 (2018) 391–406. doi:10.1016/j.ijhydene.2017.11.047.
[120] I.V. Zenyuk, D.Y. Parkinson, G. Hwang, A.Z. Weber, Probing water distribution in compressed fuel-cell gas-diffusion layers using X-ray computed tomography, Electrochemistry Communications. 53 (2015) 24–28. doi:10.1016/j.elecom.2015.02.005.
[121] C. Hartnig, I. Manke, R. Kuhn, S. Kleinau, J. Goebbels, J. Banhart, High-resolution in-plane investigation of the water evolution and transport in PEM fuel cells, Journal of Power Sources. 188 (2009) 468–474. doi:10.1016/j.jpowsour.2008.12.023.
[122] I. Manke, C. Hartnig, M. Grünerbel, W. Lehnert, N. Kardjilov, A. Haibel, A. Hilger, J. Banhart, H. Riesemeier, Investigation of water evolution and transport in fuel cells with high resolution synchrotron x-ray radiography, Appl. Phys. Lett. 90 (2007) 174105. doi:10.1063/1.2731440.
[123] A. Turhan, K. Heller, J.S. Brenizer, M.M. Mench, Passive control of liquid water storage and distribution in a PEFC through flow-field design, Journal of Power Sources. 180 (2008) 773–783. doi:10.1016/j.jpowsour.2008.02.028.
[124] J.P. Owejan, J.J. Gagliardo, J.M. Sergi, S.G. Kandlikar, T.A. Trabold, Water management studies in PEM fuel cells, Part I: Fuel cell design and in situ water distributions, International Journal of Hydrogen Energy. 34 (2009) 3436–3444. doi:10.1016/j.ijhydene.2008.12.100.
[125] P. Boillat, E.H. Lehmann, P. Trtik, M. Cochet, Neutron imaging of fuel cells – Recent trends and future prospects, Current Opinion in Electrochemistry. 5 (2017) 3–10. doi:10.1016/j.coelec.2017.07.012.
[126] Y. Wu, J.I.S. Cho, X. Lu, L. Rasha, T.P. Neville, J. Millichamp, R. Ziesche, N. Kardjilov, H. Markötter, P. Shearing, D.J.L. Brett, Effect of compression on the water management of polymer electrolyte fuel cells: An in-operando neutron radiography study, Journal of Power Sources. 412 (2019) 597–605. doi:10.1016/j.jpowsour.2018.11.048.